RESTRICTED INVESTIGATION REPORT 1691R

CSIRO

INSTITUTE OF ENERGY AND EARTH RESOURCES

DIVISION OF MINERAL PHYSICS AND MINERALOGY

MAGNETIC PROPERTIES OF IRONSTONES AND HOST ROCKS FROM THE TENNANT CREEK AREA

D.A. CLARK AND C. TONKIN

P.O. Box 136,
North Ryde, N.S.W.
Australia 2113

November, 1987

CSIRO

Division of Mineral Physics and Mineralogy
Delhi Road, North Ryde, NSW, Australia

A Division of the Institute of Energy and Earth Resources

CHIEF
Dr B. J. J. Embleton

PO Box 136, North Ryde, NSW, Australia 2113
Telephone (02) 887 8666
Telex AA25817
Facsimile (02) 887 8909

POLICY ON RESTRICTED INVESTIGATION REPORTS

Restricted Investigation Reports issued by this Division deal with projects where CSIRO has been granted privileged access to research material. In return for this access, they provide recipients with an opportunity to take advantage of results obtained on their samples or problems. Initially, circulation of Restricted Investigation Reports is strictly controlled, and we treat them as confidential documents at this stage. They should not be quoted publicly, but may be referred to as a "personal communication" from the author(s) if my approval is sought and given beforehand.

The results embodied in a Restricted Investigation Report may eventually form part of a more widely circulated CSIRO publication. Agreements with sponsors or companies generally specify that drafts will be first submitted for their approval, to ensure that proprietary information of a confidential nature is not inadvertently included.

After a certain period of time, the confidentiality of particular Restricted Investigation Reports will no longer be an important issue. It may then be appropriate for CSIRO to announce the titles of such reports, and to allow inspection and copying by other persons. This procedure would disseminate information about CSIRO research more widely to Industry. However, it will not be applicable to all Restricted Investigation Reports. Proprietary interests of various kinds may require an extended period of confidentiality. Premature release of Restricted Investigation Reports arising from continuing collaborative projects (especially AMIRA projects) may also be undesirable, and a separate policy exists in such cases.

You are invited to express an opinion about the security status of the enclosed Restricted Investigation Report. Unless I hear to the contrary, I will assume that in eighteen months time I have your permission to place this Restricted Investigation Report on open file, when it will be generally available to interested persons for reading, making notes, or photocopying, as desired.

B.J.J. Embleton.
CHIEF OF DIVISION

November, 1987

Distribution List

	Copy No.
AMIRA	1-18
CSIRO Division of Mineral Physics and Mineralogy	
D.A. Clark	19
C. Tonkin	20
P.W. Schmidt	21
B.J.J. Embleton	22
CSIRO IEER Records	23-24

This is copy number 21 of 24.

CONTENTS

LIST OF FIGURES

FIG. 7 Magnetic fabric of Explorer 50 host rock samples. Lamprophyre samples are indicated by bars on the plotted susceptibility axes. Equal area projection.

FIG. 8 Zijderveld plots for representative sedimentary specimens from Explorer 50.

FIG. 9 Soft remanence components isolated from Explorer 50 sediment samples. Equal angle projection.

FIG. 10 Hard remanence components isolated from Explorer 50 sediment samples. Equal angle projection.

FIG. 11 Palaeopole positions corresponding to the hard and soft remanence components from Explorer 50. The 1.8-0.6 Ga Precambrian apparent polar wander path for Australia (after Idnurm and Giddings, 1987) is shown for comparison. The dashed circles represent 95% cones of confidence about the pole positions. The corresponding antipoles are indicated in parentheses.

FIG. 12 Soft remanence components from Argo ironstone specimens. Equal angle projection.

FIG. 13 Magnetic fabric of the Argo mine sediment samples. Equal area projection.

FIG. 14 Magnetic fabric of specimens from Explorer 46 sediment samples. Equal area projection.

FIG. 15 Magnetic model for the West Gibbet ironstone.

FIG. 16 Magnetic fabric of West Gibbet sediment specimens. Equal area projection.

FIG. 17 Demagnetisation curve (normalised remanence intensity versus cleaning treatment) for Eldorado specimen 141B.

FIG. 18 Demagnetisation curve for Eldorado specimen 186B.

FIG. 19 "Formation mean" soft remanence components carried by magnetic sediment samples.

FIG. 20 Magnetic fabric of sediment specimens from Explorer 79 and Explorer 99.

FIG. 21 Low field thermomagnetic (susceptibility versus temperature) curves for Peko gossan samples.

FIG. 22 Demagnetisation curve for a representative specimen from the Peko gossan.

1. INTRODUCTION

The geology of the Tennant Creek region has been described by Crohn (1975) and Dodson and Gardener (1978). Recent geochronological investigations have been described by Black (1977, 1984) and Blake (1984) has presented a revised stratigraphy of the region.

The Lower Proterozoic Warramunga Group hosts economic gold-copper-bismuth mineralisation of the Tennant Creek area and consists of at least 3000m of mainly turbiditic greywacke, siltstone and shale, with interbedded felsic volcanics. The Warramunga Group is thought to have been deposited at ~1870 Ma. Penecontemporaneous greenschist facies metamorphism, deformation and mineralisation took place at ~1810 Ma. During this tectonothermal event the Warramunga Group was tightly folded about predominantly east-west axes, usually with development of an axial plane cleavage. The folded, metamorphosed sediments were subsequently eroded before deposition of the uncomformably overlying Hatches Creek Group, to the south, and the Tomkinson Creek beds, which are exposed north of Tennant Creek and can be correlated with the middle and upper parts of the Hatches Creek Group. The entire sequence was mildly metamorphosed and refolded prior to granite intrusion of the Hatches Creek Group at ~1640 Ma. The Proterozoic rocks are overlain unconformably by flat-lying Cambrian sediments.

The sedimentary sequences are intruded by a variety of igneous bodies, including granites, quartz-feldspar porphyries, dolerites and lamprophyres. The youngest thermal event evident in isotopic data is at ~1330 Ma. The mineralisation pre-dates some granites and post-dates others and is not clearly related to magmatism. Large (1975) suggests that mineralising fluids were released from the argillaceous sediments of the Warramunga Group and were channelled into anticlinal sites, ascending within zones parallel to axial surfaces. Mineralisation was deposited when the ascending fluids came into contact with a favourable carbonate-bearing horizon, producing elongated, pipe-like bodies, lying in the cleavage plane and generally also flattened within the cleavage. Solomon et al. (1987) postulate a similar syntectonic genesis for the orebodies of the Tennant Creek and Cobar (N.S.W.) areas.

The economic gold-copper mineralisation of the Warramunga Group is confined to the Carraman Formation (informal name), which consists of felsic greywackes and shales, haematitic shales and felsic tuffs, and magnetite-rich (2-15 wt %) siltstones and greywackes. The ore grade mineralisation frequently occurs juxtaposed to a thin layer of silicate facies banded iron formation and a carbonate-bearing haematitic shale unit. The magnetite in the magnetic sediments appears to be graded, suggesting that it is detrital. However the magnetite grain size is similar to the quartz grain size within each bed, which is inconsistent with a depositional feature, given the disparity in specific gravity of magnetite and quartz. The magnetite is in fact diagenetic, with grain size controlled by the interstices between quartz grains. Gold-copper-bismuth bodies occur within quartz-magnetite and quartz-haematite "ironstones", surrounded by chlorite-magnetite alteration zones. The ironstones are metasomatically zoned and transgress bedding, consistent with epigenetic mineralisation resulting from hydrothermal activity. The ore pods and their enclosing ironstones typically take the form of lenticular or pipe-like bodies, somewhat flattened within the axial plane cleavage, which can be represented quite well by triaxial ellipsoids. The long axes lie within the cleavege and tend to be either sub-horizontal, oriented east-west (parallel to the fold axes) or steeply plunging. Sub-vertical alteration pipes underlie the ironstones, plunging within the axial surface.

Because of the strong magnetic response of most of the ironstones, geophysical exploration for buried orebodies has relied almost exclusively on magnetic surveys, with many notable successes. The ellipsoid model is particularly appropriate for interpretation of magnetic anomalies due to ironstones of the Tennant Creek Field, for several reasons (Farrar, 1979):

(i) the flexibility of the model, which allows a wide variety of shapes and orientations to be considered and enables optimal targetting of drill holes,

(ii) the shapes of the ironstone bodies, which can generally be matched quite well by traixial ellipsoids,

(iii) the importance of self-demagnetisation, because of the high susceptibility of the ironstones. Self-demagnetisation significantly modifies the magnitude and direction of induced and remanent magnetisations, and hence the magnetic signature, depending on the shape of the body. The effects of self-demagnetisation can be rigorously and analytically calculated only for ellipsoidal bodies.

Because some ironstones in the Tennant Creek Field have very high gold grades they are attractive targets, even when deeply buried. This means that the initial magnetic interpretation is crucial in targetting drill holes to intersect small discrete bodies at considerable depth. In many places large volumes of magnetic sediments produce substantial anomalies, distorting the signatures of discrete ironstones within them. Knowledge of the magnetic properties of the ironstones and host rocks serves to constrain and improve the interpretation, thereby minimising the drilling required to adequately test anomalies. Down-hole vector magnetometry (Hoschke, 1985), coupled with magnetic property measurements on oriented drill-core samples, should significantly improve the efficiency of anomaly testing.

Details of the samples studied in this investigation are given in the Appendix. All samples were supplied courtesy of Geopeko. Oriented block samples of ironstone and host rocks were collected from underground drives at the Warrego and Argo mines. Oriented drill-core samples of host rocks from West Gibbet, Explorer 50, Eldorado, Explorer 142, Explorer 46 (Argo), Explorer 79 and Explorer 99 were studied, together with partially oriented full core samples of host rocks and unoriented split core samples of ironstone from a number of other prospects. Oriented block samples were also collected from the magnetic cappings of gossans associated with shallow ironstones at the Peko mine and Explorer 205.

2. EXPERIMENTAL METHODS

Several specimens (nominally 2.5cm dia. by 2.2 cm ht.) were prepared from each sample to provide duplicate analyses and to supply material for a variety of palaeomagnetic cleaning techniques. The bulk susceptibility and the bulk susceptibility variation with temperature determinations were measured on the CSIRO susceptibility/furnace instrument (Ridley and Brown, 1980). The

magnetic remanence was measured on a CTF cryogenic magnetometer or a Digico flux gate spinner magnetometer and the Digico anisotropy (of susceptibility) delineator was used to determine magnetic fabric. The CSIRO non-magnetic furnace was used for step-wise thermal demagnetisation whilst the Schonstedt GSD-1 demagnetiser was used for alternating field demagnetisation.

The sample mean magnetisations and susceptibility ellipsoids were calculated from the measured properties of the constituent specimens by vectorial and tensorial addition respectively. NRM directions and susceptibility axes are plotted on equal angle (Wulf net) and equal area (Schmidt net) stereograms respectively. Palaeomagnetic cleaning data are presented using orthogonal projections (Zijderveld plots). These methods of presentation have been described by Schmidt and Clark (1985).

3. WARREGO OREBODY AND HOST ROCKS

3.1 Geology

Goulevitch (1975) described the geology of the Warrego orebody and Farrar (1979) detailed the history of geophysical investigation of the Explorer 5 magnetic anaomaly and the detailed magnetic modelling of the Warrego ironstone body and associated pods, which produce the anomaly. The orebody has now been mined out and the geological description needs to be revised in the light of information which has emerged since 1975 (B. Williams, pers. comm.).

The main orebody consists of a major flattened pipe of magnetite and quartz-magnetite containing irregular dispersions of sulphides, chiefly chalcopyrite, pyrite and bismuthinite, and some gold. The main pipe extends from 140m below the surface to 750 m, resulting in an overall length of 860 m when the plunge of ~45° towards the SE is taken into account. The plane of flattening is tilted anticlockwise from the vertical when looking up-plunge and has strike 151° with a dip of 66° NE.

The ironstone consists of massive magnetite, containing small amounts of quartz and chlorite and variable amounts of sulphides, and quartz-magnetite, containing 10-60% quartz ± sulphides. Other lode types occurring in small pockets include quartz-haematite and chlorite-magnetite (chlorite 10-70%).

The host rocks can be divided into three sequences: phyllitic greywackes and shales west of the Footwall Fault, the footwall chloritic slates and chlorite-spotted slates and the hanging wall slate porphyroid sequence. The mineralisation is faulted but appears to have formed later than the slaty cleavage. The hydrothermal chlorites in cleaved rocks show no preferred orientation.

Although the cleavage in the Warramunga Group is generally E-W and subvertical, Warrego lies in a megakink zone, about 10km wide, within which structural trends are rotated ~45° clockwise (B. Williams, pers. comm.). The mean strike of cleavage within this zone is ~319°, compared to 275° outside the megakink. In the immediate vicinity of Warrego, however, the cleavage has been rotated even further. The average strike is ~20° and the cleavage dips ~50°ESE. The atypical orientation of the Warrego ironstone pipe (plunging at 45° within the cleavage) may reflect the tectonic event which produced this structural complexity. Continued mapping has failed to reveal evidence for the folding postulated by Goulevitch (1975). The sequences above the Footwall Fault, containing the ironstone, are easterly dipping (mean strike and dip: ~350°, ~60°E). Below the Footwall Fault some small folds have been observed. The mean bedding attitude is strike = 54°, dip = 45°SE.

3.2 Magnetic Properties

A total of 10 oriented block samples were collected from the ironstone on 5 Level, 12 Level and 14 Level, as well as 13 samples of sediments from 14 Level. The basic magnetic properties (bulk susceptibility, natural remenent magnetisation (NRM) and Koenigsberger ratio) of the oriented ironstone samples are listed in Table 1. The properties of the two quartz-magnetite and 13 sediment samples collected from 14 Level are summarised in Table 2.

The samples are all strongly magnetic, apart from the quartz-haematite sample (site 3) which is moderately magnetic. The two samples from a quartz-magnetite zone on 14 Level are among the most magnetic of the samples. The results indicate that the remanence direction is fairly consistent throughout the sampled portions of the ironstone. The NRMs have steep negative (upward) inclinations, with the exception of the quartz-haematite sample. Remanence is an important, although not dominant, contributor to the total magnetisation of

the ironstone body because of the substantial remanence intensity and consistent direction throughout. The vector mean remanence calculated from all 10 ironstone samples has intensity 18,870γ and is directed roughly west and steeply upwards (dec=284°, inc = -74°). This direction is distinctly steeper than the present field and the direction of induced magnetisation (which is deflected towards the up-plunge direction by self-demagnetisation). The NRM, therefore, is not simply a recently acquired viscous magnetisation.

Provided the sampling is representative of the ironstone body and the measured NRMs are uncontaminated by palaeomagnetic noise, the mean susceptibility (0.6012 G/Oe) and mean remanence vector represent unbiased estimates of the bulk properties of the ironstone. In reality, the sampling is probably selective, with magnetite-rich samples being favoured. Thus the susceptibility and remanence intensity may be overestimated somewhat. The consistency of NRM directions and palaeomagnetic cleaning data suggest that palaeomagnetic noise is minor in these samples. The NRM directions clearly reflect ancient acquisition of remanence. The remanence direction and Koenigsberger ratio (Q ≈0.6), however, are probably representative of the ironstone.

Farrar (1979) reported susceptibilities and NRMs for seven cubical ironstone blocks, measured by rotating the samples and using a dual fluxgate apparatus. The mean susceptibility is 0.323 G/Oe. Correcting the remanence vectors for self-demagnetisation gives an estimated NRM vector of (J = 17,260γ; dec = 353°, inc = -72°). The corresponding Koenigsberger ratio is 1.0. As for the present study, the NRM direction is steeper than the internal field of the body, which lies close to the arc joining the present field direction, (5°, -51°), and the up-plunge direction (305°, -46°). The NRM directions estimated from the present study and from Farrar's differ by 19°, which is quite satisfactory agreement. The NRM intensities are similar but the mean susceptibility of Farrar's samples is lower than the value obtained in the present study.

Combining the results in Table 1 with the data in Farrar (1979), the estimated properties of the ironstone are:

$k = 0.487$ G/Oe

$\tilde{J}_{NRM} = (17{,}970\gamma;\ 312°,\ -76°)$

$Q = 0.72$

(mean of 17 samples)

The properties of the 15 unoriented ironstone samples are listed in Table 3. Most of these samples showed evidence of contamination by palaeomagnetic noise, with rapid changes of remanence intensity and direction upon cleaning in low AF fields or after thermal demagnetisation to 100-150°C. The measured NRMs may reflect drilling-induced components, primarily carried by surface grains, which are unrepresentative of the in situ magnetisation, because soaking of specimens in concentrated HCl (to dissolve surface magnetite grains) greatly reduces the remanence intensity. For this reason the NRM intensities quoted in Table 3 in fact represent the remanences measured after acid treatment.

The mean susceptibility of the unoriented ironstone samples is 0.324 G/Oe. The apparent Koenigsberger ratios are generally somewhat lower than those determined for oriented samples, but this may reflect the removal by cleaning of some of the palaeomagnetic signal along with the noise.

The magnetic properties of the unoriented samples of host rocks from Warrego are summarised in Table 4. The quartz porphyroid and quartz feldspathoid samples are very weakly magnetic whereas the mineralised and unmineralised chloritic slate samples are moderately magnetic, by normal standards. However, the magnetisation contrast between the ironstone and the host rocks is essentially equal to the magnetisation of the ironstone, because the magnetisation of the sedimentary and intrusive rocks is, by comparison, negligible. This conclusion is supported by the data on the magnetisation of sediment samples from 14 Level (Table 2). The host rocks in this part of the mine have moderate susceptibilities and the Koenigsberger ratios are quite low ($Q = 0.1 - 0.2$). Q values much less than unity appear to be typical of the host rocks.

3.3 Magnetic Fabric

The sedimentary host rocks at Warrego exhibit a well-developed magnetic fabric. Table 5 summarises susceptibility anisotropy data for the 14 Level sediment samples. Anisotropies range from 5% (A = 1.05), which is within the normal range for deformed sedimentary rocks, to 63%. (A = 1.63), which is exceptionally high. Such high anisotropies reflect a strong preferred orientation of inequidimensional magnetite grains in response to deformation.

Although preferred orientation may arise from grain growth within a previously deformed rock, producing a mimetic fabric which conforms to the fabric already developed, it is probably difficult to produce very high anisotropies in this manner. Thus the magnetic fabric is interpreted to arise from the response to deformation of pre-existing magnetite grains.

Fig. 1 shows the orientation of major and minor susceptibility axes of specimens from these samples. Minor susceptibility axes represent poles to the magnetic foliation (plane of high susceptibility, containing the major and intermediate axes). In cleaved rocks the magnetic foliation generally corresponds to the cleavage plane. Therefore the minor axes represent cleavage poles.

The cleavage poles tend to cluster about a mean direction, corresponding to the mean pole to the axial plane cleavage, which is approximately dec = 290°, inc = + 50°, but are somewhat streaked along a girdle which dips ~45° to the NW. The major susceptibility axes (magnetic lineations) are clustered around the normal to this girdle, i.e. they are well-grouped about a mean direction which plunges ~45° to the SE. The individual susceptibility ellipsoids are predominantly prolate (P>1), indicating lineation dominant fabric, and are generally strongly lineated (9 out of 13 samples have L>1.10). The overall symmetry of the magnetic fabric defined by all the samples also indicates a predominantly linear parallel fabric.

The most remarkable feature of the magnetic fabric is the coincidence of the magnetic lineation with the plunge of the orebody. In tectonites the magnetic lineation generally represents the direction of maximum extension. At Warrego the girdle distribution of minor axes represents either variable overprinting of an earlier (bedding parallel?) foliation by a cleavage-

parallel foliation, or local variation in azimuthal orientation of the axial plane about a common axis (the lineation). In either case the normal to the girdle, i.e. the lineation, corresponds to the macroscopic fold axis.

The relationships between the magnetic fabric and the structure may be summarised as follows:

(i) Major susceptibility axes are clustered around the orebody plunge direction, which coincides with the inferred axis of folding and the direction of maximum extension. This suggests that the attitude of the orebody might have been predictable from the magnetic fabric of oriented host rock samples collected during initial drilling, prior to intersection of the ironstone.

(ii) Minor susceptibility axes exhibit an elliptical distribution centred on the average cleavage pole and elongated along the girdle normal to the lineation. Therefore the magnetic fabric defines both the axial plane and plunge of folding at Warrego.

(iii) The strong preferred orientation of the magnetite grains indicates intense deformation. The alignment of the orebody long axis, the fold axis and long axes of individual magnetite grains within the sediments is consistent with structurally controlled, syntectonic genesis of the mineralisation.

3.4 Magnetic Modelling

The discovery of the Warrego orebody can be regarded as a classic case study of magnetic interpretation using the ellipsoid model (Farrar, 1979). It is instructive to review the magnetic signature of the orebody in the light of the measured magnetic properties, thereby comparing the bulk magnetisation of the entire volume of ironstone with the magnetisation determined from measurements of small samples. This enables the number of samples required to characterise adequately the bulk properties to be roughly estimated and also serves as a test of statistical procedures for estimation of average properties from limited sampling.

Farrar (1979) modelled the Warrego orebody with an ellipsoid which totally enclosed the somewhat irregular boundary of the ironstone. Assuming magnetisation by induction with an effective susceptibility of 0.538 G/Oe gave an almost perfect match to the observed anomaly. A circumscribing ellipsoid, however, clearly overestimates the volume of ironstone. For quantitative comparison of measured magnetic properties with the bulk magnetisation deduced from modelling it is, therefore, more appropriate to model the orebody with an ellipsoid which is estimated to be the "best-fit" to the mapped boundary.

Fig. 2 shows the circumbscribing and estimated "best-fit" ellipsoids, projected onto the vertical plane containing the long axis of the orebody (the plunge plane), together with the observed and calculated vertical field anomalies. The theoretical anomally corresponding to the vector mean total magnetisation determined from the samples collected for the present study is indicated by the dots. The anomaly corresponding to Farrar's magnetic property measurements is indicated by the crosses. It appears that the magnetisation is slightly overestimated by the present study and slightly underestimated by Farrar's measurements. The combined vector mean magnetisation given in section 3.2 gives an excellent match to the observed profile. We conclude that the sampling in both cases was reasonably representative and that ~10 judiciously chosen samples are adequate to characterise the bulk properties approximately and ~20 samples are required to characterise the properties very well.

Quantitative modelling using the measured magnetic properties places quite firm constraints on the volume of the orebody. The volume of the model is 2.8×10^6 m^3, which corresponds to a total mass of $\sim 1.4 \times 10^7$ tonnes, assuming an average density of 5.0 tonnes/m^3 for the ironstone. This estimate of total tonnage agrees quite well with the value deduced from mine sections and production figures. Thus, although useful estimates of tonnage cannot generally be obtained from magnetics, it may be feasible to interpret the approximate size of Tennant Creek ironstone bodies from their anomalies. Such information may be important in assessing the economic potential of an unintersected ironstone, even though grades cannot be estimated. There are three main reasons why magnetics could be useful for estimating orebody size at Tennant Creek:

(i) the relative homogeneity of the orebodies, which produces quite homogeneous properties, both within and between orebodies. The bulk of the ironstone consists of semi-massive to massive magnetite so the variations in mgnetite content are minor compared to the rock types which give rise to most magnetic anomalies, for which magnetite is an accessory mineral with a very inhomogeneous and fairly unpredictable distribution. Such moderately magnetic rock types often exhibit variations on magnetite content of at least two orders of magnitude, from geological province to province, or even locally.

(ii) the very high intrinsic susceptibility of the ironstones, which implies that the induced magnetisation is controlled by self-demagnetisation. The effective susceptibility along an axis of the body is $k/(1 + Nk)$, where k is the intrinsic susceptibility and N is the demagnetising factor along the axis, which has an upper limit of $1/N$ for $k \to \infty$. Provided the volume fraction of magnetite, f, is high, so that $k \gg 1/N$, there is only a weak dependence of the effective susceptibility on f and the intrinsic susceptibility of the magnetite grains. Because induced magnetisation is generally about 50% of the total magnetisation, the variability in the total magnetisation is damped by self-demagnetisation.

(iii) the ironstones are generally discrete bodies within relatively weakly magnetic host rocks. Thus the total magnetic moment of the ironstone can in principle be interpreted from the anomaly associated with it. Since reasonable estimates of bulk magnetisation can be made, the approximate volume of the ironstone can be deduced.

This approach relies on separation of the "residual" anomaly due to the ironstone from the "regional" which arises from the basement or from heterogeneity of magnetisation of the host rocks. At some places, e.g. the Explorer 46 anomaly, the ironstone signature (the anomaly due to the Argo orebody) is buried within the broad anomaly arising from a large volume of magnetic sediments. In such cases quantitative modelling of the orebody is precluded. In favourable circumstances, however, the magnetics may give a more reliable indication of the size of an ironstone body than gravity surveys, which are commonly regarded as the only feasible geophysical means of tonnage estimation. Gravity surveys suffer from the limitations of high cost,

low signal-to-noise ratio in this environment, problems with regional-residual separation and the necessity to estimate the density contrast between the ironstone and host rocks to convert total anomalous mass to total mass.

3.5 Palaeomagnetism

Stepwise AF and thermal demagnetisation revealed the presence of a steep upward-directed remanence component, with evidence of a small hard component. The steep soft component corresponds to well-defined linear segments on the Zijderveld plots (Schmidt and Clark, 1985). Examples of Zijderveld plots for oriented ironstone specimens are shown in Fig. 3.

In most cases, these linear segments do not head directly towards the origin, indicating the presence of an underlying hard component which is, however, often not resolved. Variable amounts of randomly directed noise components, probably acquired during mining operations or after sampling, are also superimposed on the palaeomagnetic signal. In some cases the hard component appears to have been resolved and it was found to fall in the NW up octant.

Resolved components were determined by Principal Component Analysis, which produces a least squares fit of a straight line to a selected set of vector end-points (Schmidt and Clark, 1985).

The well-defined soft components directions obtained from massive magnetite and quartz-magnetite specimens are plotted in Fig.4. The mean directions for the two ore types are significantly different.

Massive magnetite (soft): dec = 356°, inc = -77°, α_{95}=13°, N =8, K =19.0
Quartz-magnetite (soft): dec = 229°, inc = -62°, α_{95}=16°, N=4, K=33.9

These mean directions are significantly steeper than the present field and the demagnetisation-deflected induced magnetisation. Thus the soft component is not a recently acquired viscous magnetisation.

The directions of resolved hard components which were obtained from massive magnetite specimens are plotted in Fig. 5. Consistent directions could not be obtained from the quartz-magnetite samples. They are quite

scattered within the NW up octant, so the mean direction is not very precisely defined:

Hard component: dec = 308°, inc = -29°, α_{95}=19°, N=11, K=6.9

The NRM of the ironstone therefore consists essentially of two ancient components: a steep upward soft component overprinting a NW shallow up hard component. This is consistent with results obtained from other ironstones and some host rocks, which will be discussed later. However the ironstone is not ideal material for palaeomagnetic study because of its intense magnetisation and locally inhomogeneous internal field. The local perturbations of the ambient field tend to produce scattered directions and probably bias the mean direction away from the true palaeofield direction at the time of remanence acquisition. It is therefore inadvisable to calculate palaeopole positions from the mean directions of remanence components.

4. EXPLORER 50 HOST ROCKS

4.1 Basic magnetic properties

A total of 17 fully oriented drill core samples of host rocks were collected from the Explorer 50 prospect. The samples included haematite shale, magnetic sediment and lamprophyre intrusives. The bulk susceptibilities, NRM vectors and Koenigsberger ratios of the samples are given in Table 6 and the NRM directions are plotted in Fig. 6.

Induced magnetisation dominates remanence for all host rock lithologies. The NRM directions are streaked between a northerly steep upward group and a SE down direction, implying that the remanence is multicomponent. The overall mean magnetisation for the host rocks, calculated on the assumption that the various rock types have been sampled in representative proportions, is:

All Host Rocks

J_{IND} = 85γ; 5°, -51°

J_{NRM} = 17γ; 94°, -34°

J_{RES} = 94γ; 20°, -54°

Q = 0.2

The mean magnetic properties of the three rock types are:

Magnetic Sediments (N = 11)

k = 1400 ± 300 μG/Oe

J_{IND} = 72γ; 5°, -51°

J_{NRM} = 18γ; 103°, +12.5°

J_{RES} = 68γ; 28°, -48°

Q = 0.26

Haematite Shale (N = 4)

k = 2700 μG/Oe

J_{IND} = 136γ; 5°, -51°

J_{NRM} = 51γ; 17°, -55°

J_{RES} = 187γ; 8°, -53°

Q = 0.38

Lamprophyre (N = 2)

k = 2600 μG/Oe

J_{IND} = 132γ; 5°, -51°

J_{NRM} = 55γ; 134°, -58°

J_{RES} = 164γ; 24°, -65°

Q = 0.42

4.2 Magnetic Fabric

The host rocks at Explorer 50 exhibit a well-defined magnetic fabric associated with a substantial susceptibility anisotropy.

The sample mean susceptibility axes are plotted in Fig. 7 and the various parameters characterising the strength of the magnetic fabric are given in Table 7. Lamprophyre samples are indicated by bars on the plotted points.

It appears from Fig. 7 that the magnetic fabric of the sediments has approximate axial symmetry with a dominant foliation, which has ~ E-W strike and dips steeply to the north. The prolateness parameter, P, is less than unity for all samples, indicating foliation dominant fabric. Major and intermediate susceptibility axes are interspersed throughout the foliation plane.

When the collection is subdivided on the basis of lithology it is apparent that the haematite shale samples tend to have steeply plunging lineations whereas the lineations of the magnetic sediment samples are generally oriented E-W and subhorizontal. The magnetic fabric of the lamprophyre samples appears to differ from that of the sediments and probably reflects flow during emplacement. The combined (tensorial mean) susceptibility ellipsoids of the sedimentary lithologies are:

Haematite Shale (N = 4)

Major	2780 μG/Oe; 355°, +72°
Intermediate	2660 μG/Oe; 239°, +8°
Minor	2470 μG/Oe; 147°, +16°

A = 1.13, L = 1.05, F = 1.08, P = 0.97

Bulk susceptibility = 2640 μG/Oe

Magnetic Sediments (N = 11)

Major	1430 μG/Oe; 82°, +15°
Intermediate	1380 μG/Oe, 321°, +63°
Minor	1170μG/Oe; 179°, +22°

A = 1.22, L = 1.04, F = 1.18, P = 0.88

Bulk susceptibility = 1330 μG/Oe

All Sediments (N = 15)

Major	1760 μG/Oe; 53°, +53°
Intermediate	1740 μG/Oe; 274°, +30°
Minor	1530 μG/Oe; 172°, +21°

A = 1.15, L = 1.01, F = 1.14, P = 0.89

Bulk susceptibility = 1680 μG/Oe

It can be seen that the true symmetry of the fabric is slightly orthorhombic, with a relatively weak magnetic lineation which plunges steeply within the north-dipping magnetic foliation plane. The magnetic foliation is interpreted as cleavage-parallel and should contain long axes of discrete ironstone bodies in this area.

4.3 Palaeomagnetism

The relatively large collection of oriented drill core samples from Explorer 50 afforded a unique opportunity to carry out a detailed study of geological events in the Tennant Creek area which have been recorded palaeomagnetically.

AF and thermal demagnetisation revealed the presence of two components of magnetisation in all sediment samples (Fig. 8). In many cases both components were fully resolved, allowing least-squares estimation of hard and soft component directions from individual specimens by Principal Component Analysis (Schmidt and Clark, 1985). Directions from specimens were combined to calculate sample mean directions which are plotted in Fig. 9 (soft components) and Fig. 10 (hard components). The soft component directions are generally clustered about an E, very steep up mean direction, but there are several

outlying directions. Exclusion of the outliners (defined as those directions >30° from the mean) makes very little difference to the mean direction but reduces the radius of the core of confidence significantly. The "formation mean" direction calculated from the sample mean directions (excluding outliners) is:

(Soft) dec = 98°, inc = -80°, α_{95} = 9°, N = 12, K = 24.5,

The corresponding pole position is: Lat = 16°S, Long = 114°E, A_{95} = 17°.

The sample mean directions from samples with well-resolved hard components are well grouped about a mean direction which is ESE with moderate positive inclination:

(Hard) dec = 102°, inc = +43°, α_{95} = 10°, N = 6, K = 49.0,

The corresponding palaeopole position is: Lat = 19°S, Long = 203°E, A_{95} = 10°.

These pole positions and their antipoles, which are equally valid solutions for the palaeopole positions, are plotted on the relevant portion of the Australian Precambrian pole path (Fig. 11) which is taken from Idnurm and Giddings (1987). The above-cited pole position for the hard component lies close to the portion of the track with an approximate age of 1800 Ma, whereas the antipole lies off the track altogether. This suggests that the hard magnetisation component was acquired at ~1800 Ma, which is significantly after deposition but corresponds well to the time of cooling following the peak metamorphism at 1810 Ma. The above-cited pole for the soft component and its antipole both fall on the track at ~ 1650 Ma and ~1100 Ma respectively. Black (1977, 1984) discusses the U-Pb and Rb-Sr geochronology of the Tennant Creek area and concludes that there was a major resetting of Rb-Sr systems at ~1650 Ma associated with the last apparent igneous activity in the Tennant Creek Inlier. The youngest Rb-Sr event recorded in the area is at ~1330 Ma. A lower concordia intercept age of 250 Ma from zircons which was interpreted by Black (1984) as reflecting zircon dilation and lead loss associated with final uplift in the Late Palaeozoic is now recognised as an artefact of weathering

(L. Black, pers. comm.). Thus the most likely age for the soft remanence component is ~1650 Ma, penecontemporaneous with a widespread isotopic resetting event.

We conclude that the magnetite-bearing sediments at Explorer 50 appear to have faithfully recorded two regional thermal events at ~1800 Ma and ~1650 Ma. Similar remanence components may be expected from other parts of the Tennant Creek area, provided the magnetic carriers in the rocks are palaeomagnetically stable.

5. ARGO OREBODY AND HOST ROCKS

5.1 Magnetisation of rocks from the Argo Mine and Explorer 46

The Argo orebody is a small magnetite pod lying within an extensive zone of magnetic sediments. The ironstone plunges steeply within the north-dipping cleavage plane. The broad magnetic anomaly which was known as Explorer 46 is mainly due to the sediments and the contribution due to the deep ironstone body is buried within the diffuse magnetic signature of the sediments. Thus Argo was an exceptionally difficult target and luck certainly played a part in its discovery. Knowledge of the magnetic properties of the magnetic sediments and ironstones may aid drill-hole targetting in similar difficult environments, particularly in conjunction with down-hole magnetics.

Two oriented blocks were collected from the Argo ironstone on 4 Level and 5 Level and seven oriented block samples of sediments were collected from 3 Level, 4 Level and 5 Level. The NRM vectors, induced magnetisations and resultant magnetisation of the samples are given in Table 8. Five oriented drill core samples of magnetic sediments were also provided. Their magnetic properties are given in Table 9.

The NRM of the ironstone samples is steep up, but has southerly declination in contrast to the generally N-NW declinations of Warrego ironstone samples. This may reflect deflection of the NRM vectors towards the long axes of the bodies by self-demagnatistation. The Koenigsberger ratio indicates that remanence is an important contributor to the total

magnetisation of the ironstone (Q ~ 1) and that the resultant magnetisation is very steep. The mean susceptibility of the two samples is 0.484 G/Oe.

The mean susceptibility of the Argo mine sediment samples is 1560 μG/Oe, which is similar to the susceptibility of sediments away from the orebody (1340 μG/Oe). The remanence of the host rocks is not very intense, but augments the apparent susceptibility by 10-40% (Q = 0.1 - 0.4), as it is almost parallel to the present field.

5.2 Palaeomagnetism

The remanence of the Argo ironstone samples is dominated by a soft upward-directed component, with only a hint of an underlying hard component which cannot be resolved. The directions of soft components determined by PCA are plotted in Fig. 12. The mean direction is:

Argo ironstone soft component

dec = 164°, inc = -61°, α_{95} = 35°, N = 4, K = 8.0.

The Argo mine host rocks exhibit two components, which are not always fully resolved. PCA yielded fairly well-grouped soft components which are clustered around the present field direction and rather scattered hard components (when they could be resolved at all). The mean directions are:

Argo host rock soft component

dec = 1°, inc = -50°, α_{95} = 7°, N = 36, K = 14.3,

Argo host rock hard component

dec = 323°, inc = -38°, α_{95} = 30°, N = 10, K = 3.64.

The soft component is parallel to the present field and may represent a recently acquired viscous remanence. The hard component is statistically indistinguishable from the hard component of the Warrego ironstone. Thus a similar hard component is carried by magnetite grains of different ages (early diagenetic and synmetamorphic). The hard component is also approximately antiparallel to the well-defined hard component from the Explorer 50 host rocks, but is (statistically) significantly different after conversion to

common polarity. Taken together, the results reinforce the interpretation of the ubiquitous hard component, which is present in both ironstone and host rock samples from widely separated localities, as a thermal overprint reflecting a regional event. However the time of remanence acquisition appears to vary from place to place, consistent with blocking during slow cooling. The duration of remanence acquisition corresponds to a time scale of significant apparent polar wander (to account for the difference in directions), i.e. tens of millions of years, which is much longer than the time scale of polarity reversal (~1 Ma).

5.3 Magnetic Fabric of Host Rocks

The mean susceptibility ellipsoids of the Argo sediment samples are given in Table 10 and the susceptibility axis directions are plotted in Fig. 13. The susceptibility axes of individual specimens from the Explorer 46 drill core samples are plotted in Fig. 14. In the mine the anisotropies range from 7% (A = 1.07), which is typical of low-grade sediments, to 62% (A = 1.62), which is very high. The mean susceptibility ellipsoid has an anisotropy of 34%. The magnetic fabric is foliation-dominant (P<1) with well-defined foliation poles clustered around the mean cleavage pole for the area (Fig. 14).

The mean magnetic foliation poles (minimum susceptibility axes) are similar for the samples near to (Fig. 13) and far from (Fig. 14) the orebody, although the mean magnetic foliation plane in the mine appears to have a dip which is ~15° shallower than in the drill hole intersection. In the mine, the foliation poles also appear to be somewhat streaked along a girdle which has a normal plunging steeply NNW. The drill core samples have well-grouped magnetic lineations plunging steeply NNE. The overall symmetry of the fabric at this locality suggests a lineation plunging steeply approximately towards the north, i.e. sub-parallel to the ironstone. As at Warrego, the magnetic fabric of oriented drill core samples would have predicted a probable plunge direction for the orebody prior to intersection. This information would be very valuable for improving the chances of hitting such a small deeply buried target.

6. WEST GIBBET IRONSTONE AND SEDIMENTS

6.1 Introduction

The discovery of the West Gibbet ironstone body has been discussed by Hoschke (1985). This body, which is located about 5km west of Tennant Creek and lies beneath about 150m of cover, produces a 900γ anomaly at the surface which is somewhat perturbed by the presence of magnetic sediments. Drilling indicates a geometry which is relatively equidimensional in a N-S section, but which is somewhat elongated E-W. Some thin north-dipping ironstone veins project beneath the main ironstone mass. The general geometry was further constrained by down-hole vector magnetometry.

6.2 Basic Magnetic Properties

A total of 12 unoriented split-core samples of ironstone and two oriented drill-core samples of magnetic sediments were collected. The bulk susceptibility, remanent intensity and Koenigsberger ratio of the ironstone samples are listed in Table 11. Except for one quartz-haematite sample (769m) the ironstone samples are strongly magnetic. The mean susceptibility of all ironstone samples is 0.186 G/Oe, which is significantly lower than the values determined for Warrego, Argo and several other ironstones. The Q values of individual samples range from 0.4 to 1.7, indicating that remanence may be an important contributor to the total magnetisation, depending on the consistency of NRM directions throughout the ironstone. It is not possible to estimate the vector mean NRM and the corresponding effective Koenigsberger ratio directly for these unoriented samples. However the NRMs of oriented samples from other ironstones are fairly well-grouped and the effective remanence intensity (i.e. the intensity of the vectorial mean) is typically about 90% of the arithmetic mean of the sample intensities. This suggests that the mean intensity in Table 11 should be multiplied by a correction factor of ~0.9, to allow for scatter of NRM directions. Thus the effective Q value is estimated to be 0.86 x 0.9 = 0.77.

Drilling indicates that the mineralised zone is far from homogeneous with ironstone pockets and veins interspersed with country rock. Thus the

effective magnetisation of the orebody must be corrected for the volume of non-magnetic material within its boundaries.

The bulk susceptibilities, NRM vectors and Koenigsberger ratios of the two oriented magnetic sediment samples are given in Table 12. Induced magnetisation predominates (Q = 0.26), as for magnetic sediments elsewhere in the Tennant Creek area, and the NRM direction is directed north and is somewhat steeper than present field.

Acid leaching and AF demagnetisation of selected ironstone samples reveals the presence of minor piezoremanent components, representing palaeomagnetic noise acquired during drilling and slicing. However the measured NRMs appear to be reasonably representative of in situ magnetisation, because the palaeomagnetic noise is generally only a few per cent of the total NRM vector. The Zijderveld plots for AF and thermal demagnetisation of the ironstone samples are somewhat noisy but indicate either essentially monocomponent or two component remanences, as for Warrego and Argo.

The remanence of the oriented magnetic sediment samples is dominated by a steep upward component with evidence in some samples of an underlying hard component. For two specimens the hard component appeared to be resolved and was found to lie in the NW up octant, similar to the hard components from the Warrego ironstone and the Argo host rocks.

The mean direction of the soft components determined by PCA is: dec = 17°, inc = -63°, α_{95} = 11° (N = 8, K = 28.3).

This direction is significantly steeper than the present field, and is clearly ancient. It is interpreted as representing an overprint of similar age to the thermal event which overprinted the host rocks at Explorer 50.

6.3 Magnetic Modelling

Hoschke (1985) successfully modelled the down-hole and surface magnetic anomalies of West Gibbet using a sphere of radius 39m with a resultant magnetisation which was steeper than the present field (I = -65°). The equivalent susceptibility required to match the amplitude of the anomaly for the assumed geometry was ~0.56 G/Oe, which is much higher than the measured

susceptibilities of the ironstone, particularly when the host rock content of the body is taken into account. The high apparent susceptibility and the steep resultant inclination both suggest that remanence is making a substantial contribution to the total magnetisation.

The drill-hole intersections also indicate extension along strike and a slight elongation along an axis which plunges to the north. The total volume of the body is therefore greater than that of the sphere model, and this partly accounts for the discrepancy between the modelled apparent susceptibility and the apparent susceptibility corresponding to the measured manetic properties.

A refined model using a triaxial ellipsoid was developed. The model has a strike extent of 170m and axes of 100m and 80m in cross-section (Fig. 15). The measured susceptibilities and the remanence intensity, calculated assuming an effective Q value of 0.77, were multiplied by a correction factor representing the volume fraction of the body outline consisting of ironstone. The volume fraction of ironstone required to match the magnitude of the surface anomaly was found to be 0.357, corresponding to a susceptibility of 0.1855 x 0.357 = 0.0662G/Oe and a remanence intensity of 8140γ x 0.9 x 0.357 = 2620γ (Q = 0.77) for a homogeneous body. The total mass of the ironstone corresponding to the inferred volume is ~ 1.3 million tonnes.

Because the direction of the NRM is unknown for the West Gibbet ironstone samples, although it is inferred to be steeper than present field by analogy with other ironstones and from the modelling, it has to be assumed. Two cases were considered:

(i) the NRM of the ironstone is parallel to that of the enclosing sediments. The appropriate estimate is the unweighted mean direction of the NRMs of the two oriented samples (dec = 19°, inc = -71°).

(ii) The NRM is parallel to that of the nearest sampled ironstone, namely Argo (dec = 196°, inc =-64°).

It can be seen from Fig. 15 that both assumed directions give reasonable fits to the surface anomaly. The measured surface anomaly is in fact

perturbed by a broad "regional" due to magnetic sediments. The "residual" anomaly due to the ironstone was calculated from Hoschke's (1985) model which gives a very close fit to the down-hole anomalous vectors and is the curve plotted in Fig. 15.

We conclude that the observed anomaly can be explained by the relatively intense NRM (Q_{eff} ~0.8) of the ironstone which deflects the resultant magnetisation vector towards the vertical. The NRM is probably dominated by an ancient thermal overprint component which is steeper than present field. The form of the anomaly is affected by remanence to a greater degree than for the steeply plunging pipe-like ironstone bodies (Warrego, Argo), probably because the equidimensional cross-section produces a dipole-type signature rather than the pole-type signature of the pipe-like bodies. The magnitude of the anomaly would be overestimated if the large "porosity" of the magnetic body were not taken into account.

6.4 Magnetic Fabric

Table 13 lists the susceptibility ellipsoids of the West Gibbet magnetic sediment samples. Susceptibility axes of individual specimens from the two samples are plotted in Fig. 16. The magnetic fabric of the sediments is well-defined but the anisotropy is not particularly high (~9%). The magnetic lineation plunges very steeply within the E-W vertical foliation plane. The magnetic fabric suggests that the cleavage plane around West Gibbet is vertical. In this area the longest axis of the ironstone is parallel to the intermediate susceptibility axis, rather than the major axis.

7. MAGNETIC SEDIMENTS FROM ELDORADO, EXPLORER 79 AND EXPLORER 99

7.1 Basic magnetic properties

Oriented core samples from Eldorado (2), Explorer 79(3) and Explorer 99(2) were supplied by Geopeko Ltd. Explorers 79 and 99 lie close to the Peko Mine. The susceptibilities, NRM vectors and Koenigsberger ratios of samples from the three prospects are listed in Tables 14,15, and 16 respectively.

The NRM directions generally lie in the NE up octant, except for a haematite-rich sample from Eldorado (141m) for which the NRM is NE down. The Q values are relatively high compared to magnetic sediments around Warrego, Argo, Explorer 50 and West Gibbet. For Eldorado 141m it is exceptionally high (Q = 4.7), reflecting the haematite content. Fig. 17 shows the normalised remanent intensity of a specimen from Eldorado 141m as a function of cleaning treatment. The remanence is unaffected by AF treatment to 1000 Oe and does not greatly decrease in intensity until thermally demagnetised to >600°C. This indicates that the remanence is essentially carried by haematite only. A similar plot for a specimen from 186m (Fig. 18) shows that about 70% of the NRM intensity is carried by magnetite which is very soft to AF demagnetisation and ~30% is carried by haematite.

AF and thermal demagnetisation of the Explorer 79 and Explorer 99 samples reveals that the NRMs are essentially monocomponent or have only minor, unresolvable hard components. The soft components lie close to the present field direction and may represent recently acquired viscous remanence.

Palaeomagnetic cleaning of the Eldorado samples reveals a similar soft component carried by magnetite superimposed on quite well-defined hard components which are somewhat scattered but which all fall in the NE-SE down quadrant. The mean directions of the isolated components from these localities are:

Eldorado soft component	dec = 3°, inc = -51°, α_{95} = 18°, N = 4
Eldorado hard component	dec = 96°, inc = +56°, α_{95} = 27°, N = 7
Ex 79 soft component	dec = 15°, inc = -55°, α_{95} = 30°, N = 4
Ex 99 soft component	dec = 358°, inc = -46°, α_{95} = 10°, N = 6

The directions of soft components from all localities for which oriented samples were available are plotted in Fig. 19. It can be seen they are streaked between a direction slightly shallower than present field (lying between present field and the axial geocentric dipole field) and a direction which is significantly steeper, representing the ancient overprint

component. The hard component from Eldorado is consistent with that from Explorer 50. In general the NRMs of magnetite-bearing sediments around Tennant Creek area are expected to be dominated by the soft component and thus should be sub-parallel to the present field, as for these samples. The NRMs of haematite-rich sediments and ironstones may, however, be quite oblique to the present field, because the hard component is relatively more important.

7.2 Magnetic Fabric

The susceptibility anistropy of Eldorado 186m reflects the preferred orientation of magnetite and defines a magnetic foliation which dips ~55° to ~190°T. This probably represents the local cleavage plane. The haematite-bearing sample from 141m has no clearly defined magnetic fabric, indicating that the haematite has no preferred crystallographic orientation.

The susceptibility axes for specimens from Explorers 79 and 99 are plotted in Fig. 20. The magnetic foliations are identical for the two localities, dipping ~70° to 350°T. The magnetic lineation is subvertical for Explorer 79 and sub-horizontal (~E) for Explorer 99. It would be interesting to ascertain whether this difference is reflected in the orientation of the ironstone bodies at these localities.

8. IRONSTONE AND HOST ROCK SAMPLES FROM THE ROVER FIELD

8.1 Basic Magnetic Properties

In the Rover field which lies in the SW corner of the Tennant Creek Sheet, the Warramunga Group is buried under Cambrian cover, increasing the difficulty of siting drill holes to hit small ironstones. Unoriented split core samples of ironstone and mineralised sediments were collected from Rovers 1 and 4.

Table 17 lists the bulk susceptibilities, NRM intensities and Koenigsberger ratios of the Rover Field samples. The Q values of the magnetite-haematite lode samples tend to be higher than for ironstones in the main Tennant Creek Field. This may reflect the microstructure of magnetite. The presence of haematite intergrowths would lower the effective grain size of

the magnetite and would tend to increase the Koenigsberger ratio. Remanence may therefore be even more significant for the Rover Field ironstones than in the Main Field. The Q values for the mineralised sediments are also higher than for typical magnetic sediments in the Main Field.

9. IRONSTONE AND HOST ROCK SAMPLES FROM EXPLORERS 42, 142, 154, 157, 198

9.1 Basic Magnetic Properties

Table 18 lists the bulk susceptibilities, NRM intensities and Koenigsberger ratios of an assortment of samples from the above prospects. The only oriented sample is a drill core sample of magnetic sediment from Explorer 142, which is thought to lie in the western extension of the Rover Field on the Green Swamp Well 1:250,000 sheet. As for the Rovers 1 and 4 samples the Explorer 142 ironstones have relatively high Koenigsberger ratios ($Q \sim 1\text{-}5$). The magnetic sediments have low Q values ($Q \sim 0.2$) which are typical of sediments in the Main Field. The NRM direction of the oriented sediment sample is quite oblique to the present field (WSW with moderate negative inclination), suggesting that it has retained ancient components. The anomaly at Explorer 42, which is east of the Rover Field (near the boundary of the Bonney Well and Tennant Creek sheets), is due to BIFs which do not closely resemble Tennant Creek ironstones and which may be older. The mean susceptibility is 0.145 G/Oe and remanence may contribute significantly to the total magnetisation.

Explorers 154 and 157 lie far to the NE of Tennant Creek and the porphyry rocks intersected may be part of the basement to the Warramunga Group. The form of the anomalies was not consistent with magnetisation by induction and the measured Q values (~4) suggest that remanence dominates the magnetisation of these rocks.

Explorer 198 is a typical Main Field ironstone body, lying between Gecko and Orlando. The susceptibility of the single sample is quite high (0.535 G/Oe) and remanence makes only a minor contribution to the magnetisation. The down-hole vector anomalies and drill hole intersections can be quite well matched by a prolate ellipsoid, plunging 60° to the south, with a susceptibility of 0.3 G/Oe. The massive magnetite sample is probably

27

atypical, due to the presence of haematite in much of the ironstone which would reduce the bulk susceptibility of the body. Further sampling would be required to adequately characterise the average properties of the body, in order to model quantitatively its geometry with greater confidence.

10. GOSSAN SAMPLES FROM THE PEKO MINE AND EXPLORER 205

10.1 Introduction

In the weathered zone "primary" magnetite in ironstone bodies oxidises mainly to haematite producing the characteristic gossans which cap outcropping ironstones around Tennant Creek. Thus the gossans are expected to be much less magnetic than the unoxidised ironstone. However some puzzling features have been observed. At the Peko Mine, for example, the gossan is quite strongly magnetic at the surface, although the oxidised ironstone in the subsurface, down to the base of weathering, is weakly magnetic. At Explorer 205 large amplitude, narrow anomalies which change polarity along strike were observed over and adjacent to the exposed gossan.

10.2 Magnetic Properties of the Peko Gossan

An explanation for the magnetic properties of the Peko gossan was sought in terms of the magnetic mineralogy. The properties are summarised in Table 19. The susceptibilities are quite low except for sample 1D. However all samples bear an intense remanence and the Koenigsberger ratios are very high (15-360). The NRM directions appear to be randomly scattered.

Low field thermomagnetic (k-T) curves for three of the samples are shown in Fig. 21. Fig. 21(a) shows that the susceptibility of Peko 1A is mainly due to haematite. Both MD and SD magnetite make significant contributions, but the magnetite content must be a very small fraction of the haematite content because of the much larger susceptibility of magnetite.

On the other hand, the susceptibility of sample Peko 1B is due to a small amount of MD magnetite and a smaller fraction of fine-grained maghaemite, which breaks down on heating to >300°C. The contribution of haematite to the susceptibility is negligible. Sample Peko 1D also contains a small amount of

MD magnetite, with negligible contribution to the susceptibility by haematite. However a very unusual k-T curve (Fig. 21(c) shows a rapid rise in susceptibility between 0°C and 50°C with a gradual fall in susceptibility from 50°C to ~550°C. This behaviour may reflect the presence of a rare magnetic species, or it possibly could reflect the presence of a superparamagnetic fraction (very fine grained magnetite or maghaemite) with a very narrow size range, which all unblocks around room temperature. Some of this material is destroyed after heating to 600°C, as evidenced by the irreversibility of the thermomagnetic curve.

Palaeomagnetic cleaning of the Peko gossan samples failed to reveal the presence of any consistent palaeomagnetic components between samples. A typical demagnetisation curve (normalised intensity versus treatment) is shown in Fig. 22. Most of the remanence is carried by magnetite, but it is quite hard to AF demagnetisation, with a median destructive field of ~600 Oe. This indicates that the bulk of the remanence is carried by fine-grained magnetite in the SD-PSD range. Thermal demagnetisation produces little change in remanence direction, with or without AF pre-treatment. The most likely explanation of the large, randomly directed, remanence vectors and very high Q values is that the prominent gossan outcrop, projecting above the surrounding plain, has been struck by lightning, probably repeatedly, during its long exposure.

10.3 Optical and Microprobe Analyses of Peko Gossan Samples

In order to ascertain whether a new magnetic phase was present in these samples, Dr. J. McAndrew carried out petrographic examination and electron microprobe analysis of polished sections cut from samples 1B and 1D. His descriptions follow:

"Each polished section consists largely of haematite in a quartz gangue, the haematite being partly altered to goethite. Microscopic remnants of magnetite can show zoning of reflectivity and in extent of electron back-scattering (mean atomic number).

Haematite - The texture of the haematite differs for 1B and 1D. In each there are granular to tabular aggregates. In 1D only some aggregates

have intergrowths of tabular haematite crystals with a thin rim of faintly greyer iron oxide which also fills irregular interstices between the tabular crystals.

Fine grained porous haematite replaces subhedral magnetite crystals within quartz, preserving the magnetite morphology.

Magnetite - Isotropic remnants of magnetite are more abundant in 1B and appear to be slightly pinker in 1D. These lack exsolution lamellae of ilmenite, which accords with Ti not being detected in electron microprobe analyses. The magnetite remnants in 1B are often associated with extensive irregular areas of goethite through the haematite.

In 1D magnetite occurs as microscopic residuals with distinct zoning. A group of three larger remnants, individually up to 25μm across, was examined by optical and scanning electron microscopy followed by electron microprobe analysis.

The original crystal was subhedral magnetite in quartz (Fig. 22). The outer part has been completely replaced by porous haematite. The core magnetite is separated from the outer oxidation replacement by a composite zone, consisting of a speckled rim, ~1-2 μm thick, forming an inner margin to an intermediate rim 2 to 3 μm thick.

The intermediate zone is anomalous in that while it has an iron content intermediate between magnetite and haematite (see below), the reflectivity is slightly but distinctly lower than for either of these oxides. The higher silicon content indicated by one analysis may account for this. The intermediate zone cannot consist of a cation-deficient magnetite intermediate between magnetite and maghaemite because members of this series show an increase in reflectance from magnetite to maghaemite.

While the electron probe analyses of the core magnetite give an Fe content slightly less than that of Fe_3O_4, there is a similar slight deficiency in the Fe values obtained for the haematite. This difference thus appears to arise from a slight underestimation of the high Fe content by the instrumentation, rather than from any deficiency of iron on the core magnetite below that for stoichiometric Fe_3O_4."

Electron Microprobe Analyses

	Haematite*	Magnetite in core**	Intermediate zone	Fe_2O_3	Fe_3O_4
Fe	69.1	71.8	69.2	69.9	72.3
Si	0.10	0.10	1.7	-	-
Mn	-	-	-	-	-
O (by difference)	30.8	28.10	29.1	30.1	27.7

* mean of two close analyses

** mean of three close analyses

There is therefore no evidence of exotic magnetic phases in Peko ID. Thus it is probable that the unusual k-T curve for this sample reflects a rather special grain size distribution.

10.4 Magnetic Properties of the Explorer 205 Gossan Samples

The basic magnetic properties of the gossan samples are given in Table 20. Susceptibilities are moderate to strong (for weathered material) implying the residual content of magnetite is ~ 0.5%, and the NRMs are quite intense and randomly scattered. The Koenigsberger ratios are high to very high. Overall, the properties are similar to those of the Peko gossan except for the generally higher susceptibility.

Palaeomagnetic cleaning showed the presence of multicomponent remanence in most samples, as indicated by complex Zijderveld plots, but failed to uncover any consistency of behaviour from sample to sample. This gossan forms a prominent hill and is likely to have been struck by lightning. The noisy ground magnetic anomalies probably reflect local inhomomogeneites of magnetisation, mainly reflecting intense isothermal remanences due to lightning strikes.

11. SUMMARY AND CONCLUSIONS

11.1 Magnetic Petrophysics of Ironstones and Magnetic Sediments

Tennant Creek ironstones exhibit relatively uniform magnetic properties, which greatly enhances the utility of quantitative interpretation of the location, attitude and dimensions of the ironstone bodies. Because the targets are small and often deeply buried, but are potentially rich orebodies, drill hole targetting is difficult, particularly since the host rocks can significantly perturb the magnetic signature of the ironstones. Magnetic property measurements and down hole vector magnetometry are very useful for constraining interpretation in order to minimise expensive deep drilling.

It should be noted that the axial ratios and the size of an unintersected ellipsoidal magnetic body are not uniquely determined by its external magnetic field. In fact, confocal ellipsoids of equal dipole moment (magnetisation x volume) generate identical external anomalies. This is the generalisation of the well known ambiguity of magnetisation and radius for concentric spheres. If the magnetisation can be assumed, however, the volume and the axial ratios of a triaxial ellipsoidal body, as well as the location of the centre and the orientation of the axes, can in principle be deduced from the external anomaly. Formulae for computation of magnetic anomalies due to ellipsoidal bodies have been given by Clark et al. (1987).

Except for quartz-haematite, all sampled ironstone types have very high susceptibility. Susceptibilities of the sampled Tennant Creek ironstones range from ~0.2-0.8 G/Oe with an average of ~0.45 G/Oe. Since the effective susceptibility is controlled by self-demagnetisation the variability in susceptibility is damped. For example, the effective susceptibility of a spherical ironstone varies only from 0.11 to 0.18 G/Oe as the true susceptibility varies from 0.2 to 0.8 G/Oe. An elongated ironstone has much greater effective susceptibility along the long axis than along a short axis. Thus the induced magnetisation may be deflected significantly towards the long axis.

Remanence makes a substantial, although usually not dominant, contribution to the magnetistion of the Tennant Creek ironstones. Typically

the Koenigsberger ratio is ~1. The NRMs of the ironstones are fairly consistently directed steeply upwards, so that the resultant mgnetisation direction is subparallel to the induced magnetisation. This explains the notably successful interpretation of body orientations assuming magnetisation by induction. Quantitative interpretation of body dimensions however, requires estimates of remanence vectors as well as susceptibilities.

The host rocks to the Tennant Creek ironstones are much less magnetic than the magnetite-rich ironstone bodies. Close to the ironstones, therefore, the observed anomalies can be attributed solely to the ironstones (plus in some cases, a surrounding zone of mineralised sediments). Far from the ironstone, however, its signature may be perturbed or even swamped by the anomaly arising from a large volume of magnetic sediments. It is therefore useful to characterise the magnetic properties of the host rocks. By normal standards, the diagenetic magnetite-bearing sediments in the Warramunga Group are quite magnetic, having susceptibilites similar to those of fresh basalts. Susceptibilities of magnetic sediments are typically 500-3000 μG/Oe and the Q values are generally low (~0.2). The remanence of the host rocks is generally parallel to the present field, or slightly steeper, but in some areas, notably Explorer 50, the rocks have retained ancient remanence components which deflect the total NRM away from the present field. Mineralised sediments have very variable susceptibilities, ranging up to ~0.1 G/Oe. Haematite shale is moderately magnetic and is similar in its properties to the magnetite-bearing sediments.

It should be borne in mind that in areas where haematite is the dominant iron oxide the Koenigsberger ratios of ironstones and sediments can be quite high. In such areas remanence may produce substantial anomalies although the susceptibilities are lower than for equivalent magnetite facies rocks.

11.2 Palaeomagnetism of the Warramunga Group

Two ancient geological events appear to have been recorded palaeomagnetically by the ironstones and host rocks in the Tennant Creek area. A steep upward-directed component is initially removed by AF and thermal demagnetisation, in many cases revealing an underlying hard component, which is often difficult to resolve. In some cases the soft component may

simply represent a recently acquired viscous remanence, but in samples from several localities it is clearly different from the present field direction and from the internal field direction within the ironstones, and is therefore ancient.

At all sampled localities, except Explorer 50 and Eldorado, the NRM vectors are dominated by the soft component and are therefore subvertical. The magnetic sediments and haematite shales at Explorer 50 appear to be excellent palaeomgnetic recorders which have retained a record of two ancient geological events. In most cases AF and thermal demagnetisation clearly resolve the soft and hard components which have quite discrete (non-overlapped) coercivity and blocking termperature spectra. The hard component, which is ~E and down at Explorer 50 and Eldorado, is interpreted to represent a thermoremanence or thermochemical remanence acquired at ~1800 Ma during post-metamorphic cooling. Any earlier remanence carried by the magnetite or haematite grains appears to have been obliterated during the regional metamorphism which peaked at ~1810 Ma. A subsequent major thermal event at ~1650 Ma, which produced widespread resetting of Rb-Sr systems, appears to have also caused the ubiquitous overprinting of the remanence.

Although the general characteristics of the palaeomagnetic signatures appear to be consistent throughout the area, there appear to be systematic differences in palaeomagnetic directions from locality to locality. For the hard component both polarities are represented (~ESE and down/~WNW and up). The dual polarities, and a fortiori differences in directions, suggest prolonged acquisition of remanence, probably over tens of millions of years. This is consistent with acquisition during slow cooling, with systematic variations in the thermal environment and in the magnetic carriers at different places.

11.3 Magnetic Fabric and geological structure

The susceptibility anisotropy of the sedimentary rocks of the Warramunga Group reflects a strong preferred orientation of magnetic mineral grains which has developed in response to the deformation. The magnetic fabric therefore conveys information on the geological structure which may be a valuable aid to drill hole targetting.

In all cases the magnetic foliation is parallel to the cleavage plane. Since the elongated ironstone bodies nearly always lie within the cleavage plane, which has variable dip across the area, an independent estimate of its orientation is useful when there is no clearly visible fabric in the rocks. Furthermore the magnetic fabric generally shows orthorhombic symmetry with well-grouped major axes (magnetic lineations) and intermediate axes within the magnetic foliation plane. This fabric is interpreted to reflect the finite strain axes in the sediments with the magnetic lineation parallel to the direction of maximum extension.

The ironstones are thought to be syntectonic and their structure is probably controlled, albeit indirectly, by the deformation. It is not surprising, then, that the magnetic fabric in the enclosing sediments appears to show a clear correlation with the orientation of the enclosed ironstone body, as both are related to the deformation. This relationship is particularly clear at Warrego where the well-defined magnetic linetion, plunging to the SE, parallels the orebody plunge. The possibility that the plunge direction of an unintersected ironstone target could be predicted from the magnetic fabric of nearby sediments is an interesting potential application of magnetic property measurements which should provide further justification for routine orientation of drill core in this area.

12. ACKNOWLEDGEMENTS

We thank the staff of Geopeko, in particular Terry Hoschke, Brian Williams, Bob Love and Paul Balind, for their co-operation and encouragement of this work. John McAndrew kindly carried out petrographic examination and electron microprobe analysis of the Peko gossan samples.

13. REFERENCES

Black, L.P., 1977. A Rb-Sr geochronological study in the Proterozoic Tennant Creek Block, central Australia, BMR J. Aust. Geol. Geophys., 2, 111-122.

Black, L.P., 1984. U-Pb zircon ages and a revised chronology for the Tennant Creek Inlier, Northern Territory, Aust. J. Earth Sci., 31, 123-131.

Blake, D.H., 1984. Stratigraphic correlations in the Tennant Creek region, central Australia: Warramunga Group, Tomkinson Creek beds, Hatches Creek Group, and Rising Sun Conglomerate, BMR J. Aust. Geol. Geophys., 9, 41-47.

Clark, D.A., S.J. Saul and D.W. Emerson, 1987. Magnetic and gravity anomalies of a triaxial ellipsoid, Explor. Geophys., 17, 189-200.

Crohn, P.W., 1975. Tennant Creek - Davenport Proterozoic Basins - regional geology and mineralization, in C.L. Knight (ed.), Economic Geology of Australia and Papua New Guinea, Aust. I.M.M., Melbourne, pp. 421-424.

Dodson, R.G. and J.E.F. Gardener, 1978. Tennant Creek, Northern Territory - 1:250,000 Geological Series, Bureau of Mineral Resources Australia, Explanatory Notes 58/5314.

Farrar, L.J.D., 1979. Some comments on detailed magnetic investigations of ellipsoidal bodies at Tennant Creek, Bull. Aust. Soc. Explor. Geophys., 10, 26-33.

Goulevitch, J., 1975. Warrego cooper-gold orebody, in C.L. Knight (ed.), Economic Geology of Australia and Papua New Guinea, Aus. I.M.M., Melbourne, pp. 430-436.

Hoschke, T., 1985. A new drill hole magnetometer: preliminary results from the Tennant Creek area, Explor. Geophys., 16, 365-374.

Idnurm, M. and J. Giddings, 1987. Australian Precambrian apparent polar wander: a review, Tectonophysics (in press).

Large, R.R., 1975. Zonation of hydrothermal minerals at the Juno mine, Tennant Creek Goldfield, central Australia, Econ. Geol., 70, 1387-1413.

Ridley, B.H. and H.E. Brown, 1980. The transformer bridge and magnetic susceptibility measurement. Bull. Aust. Soc. Explor. Geophys., 11, 110-114.

Schmidt, P.W. and D.A. Clark, 1985. Presentation and analysis of palaeomagnetic data, CSIRO Restricted Investigation Report 1602R.

Solomon, M., B.L. Schmidt and J.L. Walshe, 1987. The base-metal deposits of the Cobar district, Australia - are they further examples of syntectonic, synmetamorphic ore deposits? BMR J. Aust. Geol. Geophys. (submitted).

Table 1. Magnetic properties of the oriented Warrego ironstone samples (5L, 12L, 14L).

Site	N	k	J	Dec	Inc	Q
1	7	304,300	119,400	353°	-87°	0.77
2	5	204,400	68,590	303°	-60°	0.66
3	3	2,445	3,060	340°	-24°	2.45
4	7	942,500	262,700	326°	-68°	0.54
5	8	389,600	146,900	13°	-67°	0.74
7	7	470,200	171,900	8°	-52°	0.71
8	9	534,000	96,780	348°	-50°	0.35
9	7	1,650,000	233,400	313°	-64°	0.28
14/4	6	958,800	402,400	234°	-49°	0.82
14/9	6	556,100	560,100	232°	-71°	1.97
ALL	10	601,200	188,700	284°	-74°	0.61

N = Number of vectors combined to calculate mean
k = Bulk cgs susceptibility x 10^6
J = NRM intensity in microgauss (μG)
Q = Koenigsberger ratio = J/kH, where H = 0.512 Oe

Table 2. Magnetisation of Warrego 14 Level Samples

Sample	$\tilde{J}_{NRM}$	$\tilde{J}_{IND}$	$\tilde{J}_{RES}$	Q
1	1.1; 103°,-41°	10.9; 2°, -53°	11.4; 10°, -56°	0.10
2	24; 308°, -17°	23; 1°, -51°	42; 329°, -36°	1.0
3	0.5; 111°, -84°	5.2; 3°, -50°	5.6; 4°, -54°	0.10
4	40,240; 234°, -49°	49,090; 5°, -51°	72,450; 310°, -71°	0.82
5	37; 232°, -34°	132; 356°, -51°	142; 335°, -60°	0.28
6	7; 243°, -51°	56; 2°, -53°	60; 356°, -57°	0.12
7	12; 8°, -24°	47; 356°, -49°	58; 359°, -44°	0.26
8	22; 9°, -34°	62; 0°, -48°	84; 2°, -44°	0.36
9	56,010; 232°, -71°	28,470; 5°, -51°	76,280; 297°, -79°	2.0
10	540; 207°, -25°	4210; 356°, -50°	4150; 350°, -57°	0.13
11	1.0; 160°, -30°	7.9; 3°, -49°	7.0; 7°,-51°	0.13
12	155; 198°, -24°	441; 352°, -49°	445; 332°, -66°	0.35
13	37; 26°, -56°	375; 350°, -50°	409; 352°, -51°	0.10
14	50; 213°, -64°	62; 6°, -45°	93; 344°, -73°	0.81
15	15; 184°, -33°	6; 8°, -48°	15; 182°, -56°	2.5
Ironstone combined (samples 4 and 9)	47,260; 233°, -62°	38,780*; 5°, -51°	74,350; 305°, -71°	1.2
Sediments combined	59; 209°, -34°	418; 356°, -50°	421; 349°, -57°	0.14

* equivalent to a susceptibility of 0.757 G/Oe

Magnetisations expressed as Intensity (γ); Dec, Inc (1γ = 10 μG)

Table 3. Magnetic properties of the Warrego unoriented ironstone samples.

Depth (m)	Lithology	k	J	Q
DDH (10/8060/68)				
28.7	Massive magnetite	525,000	68,900	0.26
30.1	" "	441,000	-	-
32.6	" "	178,300	77,000	0.84
46.2	Quartz-magnetite	105,200	23,000	0.43
49.7	" "	186,200	39,100	0.41
50.7	" "	431,300	-	-
70.2	Massive magnetite	678,100	42,800	0.12
75.2	" "	439,900	106,800	0.47
84.8	" "	266,300	24,900	0.18
92.4	" "	108,900	26,500	0.48
94.3	" "	526,400	35,500	0.13
103	" "	42,900	47,600	2.17
DDH (10/810/64)				
43.1	Massive Magnetite	249,900	92,200	0.72
49.9	" "	386,000	63,400	0.32
57.9	" "	299,800	-	-

k = Bulk cgs susceptibility x 10^6

J = Remanence intensity in microgauss (following acid treatment)

Q = Koenigsberger ratio

Table 4. Magnetic properties of the Warrego host rocks.

Sample depth (m)	N	Lithology	k	J	Q
1.6	4	quartz porphyroid	25	0.31	0.02
22.0)	1	quartz feldspathoid	60	0.41	0.01
22.2)	4		67	1.95	0.06
63.8)	2	mineralised chloritic	2160	240	0.22
104)	2	slate	550	60	0.21
107)	5		18,360	1010	0.11
110)	2	chloritic slate	2870	265	0.18
112)	2		560	69	0.24

where

N = Number of specimens
k = Bulk cgs susceptibility x 10^6
J = NRM intensity in microgauss
Q = Koenigsberger ratio = J/kH, where H = 0.512 Oe

Table 5. Susceptibility Ellipsoids of Warrego 14 Level Sediment Samples

Sample	Susceptibility ellipsoid	A	L	F	P
1	218; 133°, 64° 194; 229°, 3° 184; 320°, 26°	1.18	1.12	1.05	1.07
2	461; 126°, 54° 431; 24°, 9° 411; 288°, 35°	1.12	1.07	1.05	1.02
3	102; 152°, 45° 100; 27°, 30° 97; 277°, 30°	1.05	1.02	1.03	0.99
5	2810; 126°, 39° 2420; 13°, 26° 2280; 259°, 40°	1.23	1.16	1.06	1.09
6	1056; 151°, 51° 877; 59°, 2° 847; 327°, 39°	1.25	1.20	1.04	1.16
7	1025; 130°, 31° 862; 31°, 15° 813; 280°, 55°	1.26	1.19	1.06	1.12
8	1260; 148°, 34° 1140; 52°, 8° 1020; 310°, 55°	1.24	1.11	1.12	0.99
10	88,320; 116°, 49° 79,770; 13°, 11° 68,790; 274°, 39°	1.28	1.11	1.16	0.95
11	157; 157°, 30° 151; 52°, 24° 143; 290°, 50°	1.10	1.04	1.06	0.98
12	9220; 142°, 44° 6670; 40°, 12° 5640; 298°, 43°	1.63	1.38	1.18	1.17
13	7960; 136°, 48° 5980; 20°, 21° 4870; 275°, 34°	1.63	1.33	1.23	1.08

Sample	Susceptibility ellipsoid	A	L	F	P
14	1390; 200°, 12° 1250; 108°, 13° 1080; 332°, 72°	1.29	1.11	1.16	0.96
15	132; 262°, 13° 128; 354°, 11° 114; 124°, 73°	1.16	1.03	1.12	0.92

Susceptibility ellipsoids are given in the form:-
Major axis (k_1)
Intermediate axis (k_2)
Minor axis (k_3)

Susceptibilities are expressed in μG/Oe (ie k = cgs (emu) susceptibility x 10^6)

A = Degree of anistropy = k_1/k_3

L = Degree of lineation = k_1/k_2

F = Degree of foliation = k_2/k_3

P = Degree of prolateness = L/F (P>1: prolate ellipsoid, lineation dominant)

Table 6. Magnetic properties of Explorer 50 samples

Sample Depth (m)	N	k	J	Dec	Inc	Q
147.3	3	640	47.52	352°	-86°	0.15
159	2	45	7.3	171°	-70°	0.32
180.1	6	55	6.2	96°	-11°	0.22
186.7	2	970	79.8	3°	-77°	0.16
222.5	3	890	120	31°	-67°	0.26
241.2	3	1,560	263	121°	-6°	0.33
241.5	4	2,570	220	124°	-21°	0.17
244.7	2	2,140	248	114°	3°	0.23
245	3	2,820	1,805	103°	36°	1.25
246.7	4	1,680	150	116°	-73°	0.17
253.6	3	3,605	960	144°	-70°	0.52
257	2	9,320	1,930	16°	-57°	0.40
297.5	4	1,220	54.4	146°	-62°	0.09
309	3	2,165	102	84°	-66°	0.09
329.5	5	1,120	89.4	342°	-50°	0.16
372.2	2	80	1.12	292°	-74°	0.03
402	2	150	24.7	11°	-52°	0.32
Mean	17	1,665	173	94°	-34°	0.20

Where

N = Number of vectors combined to calculate mean
k = Bulk cgs susceptibility x 10^6
J = NRM intensity in microgauss
Q = Koenigsberger ratio = J/kH, where H = 0.512 Oe

Table 7. Magnetic fabric of Explorer 50 samples

Sample Depth (m)	Lithology	A	L	F	P
147.3	MS	1.28	1.04	1.23	0.84
159	HS	1.14	1.02	1.11	0.92
180.1	HS	1.55	1.24	1.25	0.99
186.7	MS	1.32	1.07	1.22	0.88
222.5	MS	1.26	1.05	1.20	0.87
241.2	La	1.11	1.02	1.08	0.94
241.5	MS	1.20	1.02	1.18	0.86
244.7	MS	1.29	1.04	1.24	0.84
245	MS	1.25	1.01	1.24	0.82
246.7	MS	1.29	1.03	1.25	0.82
253.6	La	1.10	1.02	1.08	0.95
257	HS	1.11	1.04	1.07	0.98
297.5	HS	1.24	1.03	1.20	0.86
309	MS	1.25	1.06	1.17	0.91
329.5	MS	1.26	1.04	1.21	0.86
372.2	MS	1.08	1.00	1.08	0.93
402	MS	1.15	1.05	1.10	0.95

-Susceptibility ellipsoids are given in the form:-
Major axis (k_1)
Intermediate axis (k_2)
Minor axis (k_3)

Susceptibilities are expressed in μG/Oe (ie k = cgs (emu) susceptibility x 10^6)

A = Degree of anistropy = k_1/k_3

L = Degree of lineation = k_1/k_2

F = Degree of foliation = k_2/k_3

P = Degree of prolateness = L/F (P>1: prolate ellipsoid, lineation dominant)

MS = magnetic sediment,

HS = haematite shale,

La = lamprophyre

Table 8. Magnetisation of Argo samples

Sample	$\tilde{J}_{NRM}$	$\tilde{J}_{IND}$	$\tilde{J}_{RES}$	Q
3 Level				
1	4.2; 317°, -62°	64.8; 10°, -53°	68.5; 8°, -54°	0.06
2	7.0; 0°, -42°	57.8; 11°, -55°	64.6; 9°, -53°	0.12
3	321; 130°, -47°	503; 5°, -61°	708; 62°, -72°	0.64
4 Level				
1	4.6; 348°, -62°	75.4; 10°, -51°	79.8; 9°, -52°	0.06
2	15.8; 21°, -50°	170.8; 7°, -51°	186.4; 8°, -51°	0.09
3	36,260; 190°, -39°	18,130; 8°, -42°	37,910; 192°, -67°	2.00
5 Level				
1	6.7; 350°, -46°	78.0; 10°, -53°	84.5; 8°, -52°	0.09
2	4.0; 347°, -59°	33.4; 8°, -50°	37.3; 6°, -51°	0.12
3	26,660; 341°, -79°	31,500; 1, -40°	54,670; 358°, -58°	0.85
Ironstone combined (Samples 4LS3 and 5LS3)	27,245; 196°, -64°	24,790; 4°, -41°	41,430; 345°, -80°	1.10
Sediments combined (Samples 3LS1,2,3; 4LS1,2; 5LS1,2)	6.9°; 1°, -53°	80; 9°, -52°	86.8; 8°, -52°	0.09

Magnetisations expressed as : Intensity (γ); Dec, Inc (1γ = 10 μG)

Table 9. Magnetic properties of Explorer 46 sediment samples.

Sample Depth (m)	N	k	J	Dec	Inc	Q
258	2	437	34	135°	-75°	0.15
303	2	631	87	17°	-71°	0.27
347	1	1,280	61	46°	-39°	0.09
349	3	2,540	620	345°	-49°	0.48
400	1	1,820	470	356°	-59°	0.50
Mean	5	1,340	250	354°	-56°	0.37

Where

N = Number of vectors combined to calculate mean
k = Bulk cgs susceptibility x 10^6
J = NRM intensity in microgauss
Q = Koenigsberger ratio = J/kH, where H = 0.512 Oe

Table 10. Susceptibility Ellipsoids of Argo Sediment Samples

Samples	Susceptibility Ellipsoid	A	L	F	P
3 Level					
	1392; 045°, 37°				
1	1349; 282°, 36°	1.23	1.03	1.19	0.87
	1136; 164°, 33°				
	1343; 334°, 62°				
2	1302; 072°, 4°	1.25	1.03	1.22	0.84
	1071; 164°, 28°				
	14,068; 297°, 35°				
3	12,357; 076°, 47°	1.62	1.14	1.43	0.80
	8,662; 191°, 21°				
4 Level					
	1634; 030°, 34°				
1	1579; 265°, 41°	1.07	1.03	1.05	0.98
	1400; 144°, 31°				
	3552; 044°, 28°				
2	3462; 284°, 43°	1.17	1.03	1.13	0.91
	3305; 155°, 34°				
5 Level					
	1789; 050°, 30°				
1	1712; 285°, 46°	1.22	1.04	1.17	0.89
	1467; 160°, 31°				
	663; 045°, 14°				
2	618; 293°, 56°	1.13	1.07	1.06	1.01
	585; 143°, 30°				
	3440; 299°, 40°				
Combined	3210; 072°, 39°	1.34	1.07	1.25	0.85
	2560; 184°, 26°				

Table 11. Magnetic properties of the West Gibbet ironstone.

Sample Depth (ft)	N	k	J	Q
634	1	268,000	155,900	1.14
637	1	259,800	94,300	0.71
645	1	64,000	27,400	0.84
718.5	1	499,400	120,900	0.47
719	1	336,300	255,400	1.48
769	2	170	60	0.69
785	2	82,400	15,720	0.37
771	1	237,000	140,600	1.23
772	1	159,800	40,800	0.50
790	1	140,600	42,200	0.59
794	1	122,100	24,960	0.40
820.5	2	56,900	49,900	1.7
Mean	12	185,500	81,400	0.86

N = Number of specimens
k = Bulk cgs susceptibility x 10^6
J = NRM intensity in microgauss
Q = Koenigsberger Ratio = J/kH, where H = 0.512 Oe

Table 12. Magnetic properties of the West Gibbet magnetic sediments.

Sample Depth	N	k	J	Dec	Inc	Q
270	4	470	65	356°	-65°	0.3
353	4	40	4	36°	-75°	0.2
Mean	2	257	35	357°	-66°	0.26

N = Number of vectors combined to calculate mean
k = bulk cgs susceptibility $x10^6$
J = NRM intensity in microgauss
Q = Koenigsberger ratio

Table 13. Magnetic fabric of the West Gibbet magnetic sediments.

Sample	N	Axes	Dec	Inc	k	A	L	F	P
		Max	130°	71°	482				
Mean 270	4	Int	255°	12°	466	1.09	1.03	1.05	0.98
		Min	348°	15°	442				
		Max	45°	81°	43.6				
Mean 353	4	Int	284°	5°	43.3	1.07	1.01	1.06	0.95
		Min	193°	8°	40.7				
270 and	2	Max	194°	74°	264				
353		Int	88°	5°	253	1.09	1.04	1.05	1.00
combined		Min	357°	16°	242				

Where

N = Number of ellipsoids combined to calculate mean
k = Susceptibility $x10^6$ of each axis
A = Degree of anistropy, $A = k_1/k_2$
L = Degree of lineation, $L = k_1/k_3$
F = Degree of foliation, $F = k_2/k_3$
P = Degree of prolateness, P = L/F (P>1: prolate ellipsoid, lineation dominant)

Table 14. Magnetic properties of Eldorado samples.

Sample Depth (m)	N	k	J	Dec	Inc	Q
141	4	445	1,060	44°	+50°	4.65
186	3	14,700	3,900	26°	-40°	0.52

Where

N = Number of specimens
k = Bulk cgs susceptibility $x10^6$
J = NRM intensity in microgauss
Q = Koenigsberger ratio = J/kH, where H = 0.512 Oe

Table 15. Magnetic properties of Explorer 79 sediment samples.

Sample Depth (m)	N	k	J	Dec	Inc	Q
139.6	1	404	156	76°	-62°	0.75
161.8	1	1000	100	25°	-48°	0.20
213.3	1	82	63	356°	-54°	1.50
Mean	3	495	100	40°	-60°	0.40

Where

N = Number of vectors combined to calculate mean
k = Bulk cgs susceptibility x 10^6
J = NRM intensity in microgauss
Q = Koenigsberger ratio = J/kH, where H = 0.512 Oe

Table 16. Magnetic properties of Explorer 99 sediment samples.

Sample Depth (m)	N	k	J	Dec	Inc	Q
168	3	3,160	2,000	358°	-54°	1.24
176	3	3,890	1,850	12°	-35°	0.93
Mean	2	3,525	1,890	6°	-45°	1.05

Where

N = Number of vectors combined to calculate mean
k = Bulk cgs susceptibility x 10^6
J = NRM intensity in microgauss
Q = Koenigsberger ratio = J/kH, where H = 0.512 Oe

Table 17. Magnetic properties of the Rover samples.

Sample	N	k	J	Q
Rover 1				
567	1	21,000	71,500	6.65
570.4	1	63,400	34,850	1.07
573.2	1	312,800	377,500	2.36
586	1	110,200	70,400	1.25
603	1	100	96	1.88
618	1	57	3	0.1
545	1	170	640	7.35
570	1	110	55	0.98
585	1	75	40	1.04
Rover 4				
295	1	3,800	620	0.32
312	1	142,700	50,700	0.69
329	1	1,050	2,300	4.28

Where

N = Number of specimens
k = Bulk cgs susceptibility x 10^6
J = NRM intensity in microgauss
Q = Koenigsberger ratio = J/kH, where H = 0.512 Oe

Table 18. Magnetic properties of samples from Explorers 42, 142, 154, 157, 198.

Sample	N	k	J	Q
Explorer 42				
248.3	1	170,000	274,000	3.2
274.15	2	120,000	26,300	0.4
Explorer 142 Hole 1				
439.15	4	850,000	580,000	1.3
445.0	2	95,000	112,000	2.3
Hole 2				
470.45	4	4,540	225	0.1
480.65	4	1,630	280*	0.3
Hole 3				
418.2	3	275	700	5.0
421.4	1	200,000	270,000	2.6
Explorer 154	4	145	340	4.6
Explorer 157	5	830	1,500	3.2
Explorer 198	4	535,000	97,000	0.35

Where

N = Number of specimens
k = Bulk cgs susceptibility x 10^6
J = NRM intensity in microgauss
Q = Koenigsberger ratio = J/kH, where H = 0.512 Oe
* NRM direction : dec = 240°, inc = -40°

Table 19. Magnetic properties of the Peko gossan samples.

Site	N	k	J	Dec	Inc	Q
1A	3	200	37,200	254°	36°	363
1B	5	220	15,900	180°	-4°	141
1C	3	250	9,100	25°	-19°	71
1D	3	11,700	88,300	47°	-49°	15

Where

N = Number of specimens
k = Bulk cgs susceptibility x 10^6
J = NRM intensity in microgauss
Q = Koenigsberger ratio q = J/kH, where H = 0.512 Oe

Table 20. Magnetic properties of Explorer 205 gossan samples.

Site	N	k	J	Dec	Inc	Q
1A	4	6,970	102,700	193°	-8°	29
1B	2	1,860	124,450	297°	-33°	131
1C	2	6,490	16,550	155°	25°	5.0
1D	4	2,580	19,700	253°	-11°	15.0
1E	6	3,480	43,650	235°	9°	24.5
1F	3	35,300	44,490	248°	42°	2.5
1H	3	5,400	17,150	168°	-4°	6.2
1I	3	11,500	57,760	66°	-23°	9.8

Where

N = Number of specimens
k = Bulk cgs susceptibility x 10^6
J = NRM intensity microgauss
Q = Koenigsberger ratio q = J/kH, where H = 0.512 Oe

APPENDIX - LIST OF SAMPLES

WARREGO MINE
DRILL CORE
10 Level, Hole 68, 8060N Section (10/8060/68)

UNORIENTED SAMPLES (depth in metres)	DESCRIPTION
1.6	Quartz porphyroid
22.0) 22.2)	Quartz feldspathoid
* 28.7) * 30.1) * 32.6)	Massive magnetite and sulphides
* 46.2) * 49.7) * 50.7)	Quartz - magnetite
* 63.8	Mineralised chloritic slate
* 70.2) * 75.2) * 84.8) * 92.4) * 94.3) * 103)	Massive magnetite and sulphides
* 104	Mineralised Chloritic slate
107) 110.7) 112.7)	Chloritic slate

10 Level, Hole 64, Section 810N (10/810/64)

* 43.1) * 49.9) * 57.9)	Massive magnetite and sulphides

* Indicates split core sample.

ORIENTED BLOCK SAMPLES
5 Level

WS1) WS2)	Massive magnetite and minor sulphides
WS3	Quartz-haematite

12 Level

WS5 WS7 WS8 WS9	Massive magnetite and minor sulphides

14 Level

14/1,2,3,5,6,7,8,10,11,12,13,14,15	Sediments
14/4,9	Quartz magnetite

EXPLORER 50

ORIENTED CORE SAMPLES	DESCRIPTION
DDH 3 (depth in metres)	
147.3) 186.7) 222.5)	Magnetic sediments
257	Haematite Shale
329.5) 372.2) 402)	Magnetic sediments
DDH 2A	
159	Haematite Shale
309	Magnetic Sediments
DDH 2	
180.1	Haematite Shale
241.2	Lamprophyre
241.5) 245)	Magnetic Sediments contact with lamprophyre
244.7	Magnetic sediments
246.7	Magnetic sediments
297.5	Haematite Shale
253.6	Lamprophyre

WEST GIBBET

CORE SAMPLES	DESCRIPTION
DDH 1 (depth in feet) - unoriented	
* 634	Massive
* 637	magnetite
* 645	
* 771	Chloritic
* 772	Magnetite
* 790	Siliceous
* 794	Magnetite
* 718.5	Dense fine grained
* 719	magnetite and specularite
DDH 3 (depth in feet) - unoriented	
* 769	Quartz haematite
* 785	Quartz magnetite
* 820.5	Chloritic magnetite
DDH 6B (depth in metres) - oriented	
270	Magnetic
353.1	sediments

* Indicates split core samples

ARGO

ORIENTED BLOCK SAMPLES	DESCRIPTION
3 Level	
1)	Magnetic
2)	Sediments
3)	
4 Level	
1)	Magnetic
2)	Sediments
3	Massive magnetite
5 Level	
1)	Magnetic
2)	Sediments
3	Massive magnetite

ROVER FIELD - UNORIENTED DRILL CORE SAMPLES

ROVER 1

DDH 2 WRO2 (depth in metres)	DESCRIPTION
* 567)	Magnetite - haematite lode with quartz and minor sulphides
* 570.4)	
* 573.2)	
* 586)	Mineralised Sediments
* 603)	
* 618)	

WRO3

* 545.2)	Magnetite - haematite lode
* 570)	
* 585)	

ROVER 4

DDH 3 (depth in metres)

* 295)	Magnetite - haematite -jasper/dolomite lode
* 312)	
* 329)	

EXPLORER 142

DDH 1

439.15 m	Mineralised magnetite lode
445.0 m	Quartz-magnetite lode

DDH 2

470.95 m)	Magnetic sediment
480.65 m) - oriented	

DDH 3

418.3 m	BIF
421.4 m	Magnetite lode

ELDORADO - oriented

DDH 6

141 m)	Magnetic sediments
186 m)	

EXPLORER 42 - unoriented

DDH 1

248.3 m	BIF
274.15 m	BIF - lode

* indicates split core samples

EXPLORER 46 (ARGO)

ORIENTED CORE SAMPLES (depth in metres)	DESCRIPTION
DDH 13A	
258.5	Magnetic sediments
DDH 14	
303)	Magnetic sediments
349.4)	
400)	
DDH 21	
347	Magnetic sediments

EXPLORER 79

ORIENTED CORE SAMPLES (depth in metres)	DESCRIPTION
DDH 1	
137.6)	Magnetic sediments
161.8)	
213.3)	

EXPLORER 99

ORIENTED CORE SAMPLES (depth in metres)	DESCRIPTION
DDH 1	
168.8)	Magnetic Sediments
176.7)	

EXPLORER 154

One unoriented drill core sample of porphyry

EXPLORER 157

One unoriented drill core sample of porphyry

EXPLORER 198

DDH 1

One unoriented drill core sample of massive magnetite

PEKO MINE

Four oriented block samples collected from the gossan.

EXPLORER 205

Nine oriented block samples collected from the gossan.

FIG. 1 Magnetic fabric of sedimentary host rocks from the Warrego mine.

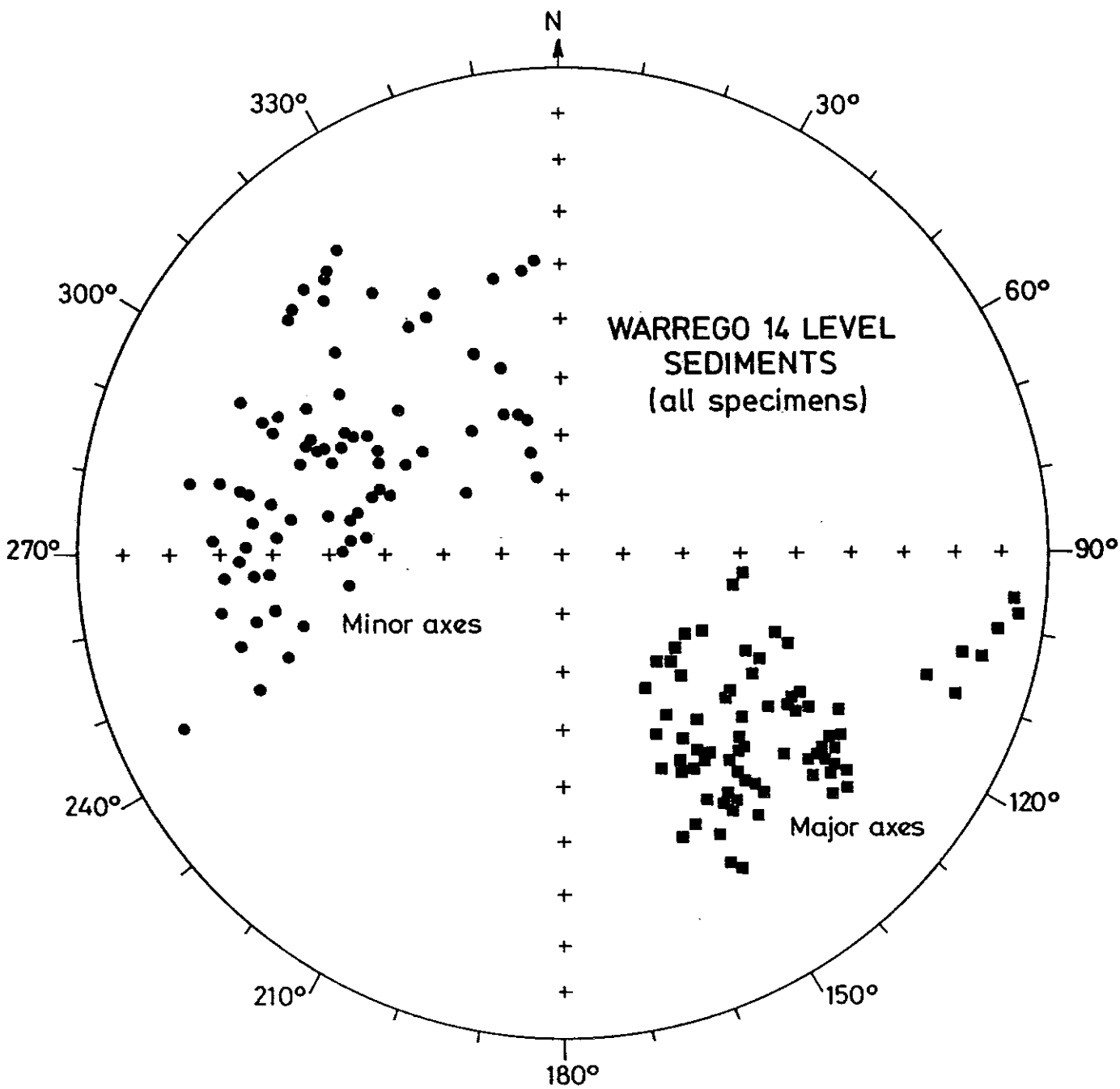
N
30°
60°
90°
120°
150°
180°
210°
240°
270°
300°
330°
WARREGO 14 LEVEL
SEDIMENTS
(all specimens)
Minor axes
Major axes

FIG.1

FIG. 2 Magnetic model of the Warrego ironstone

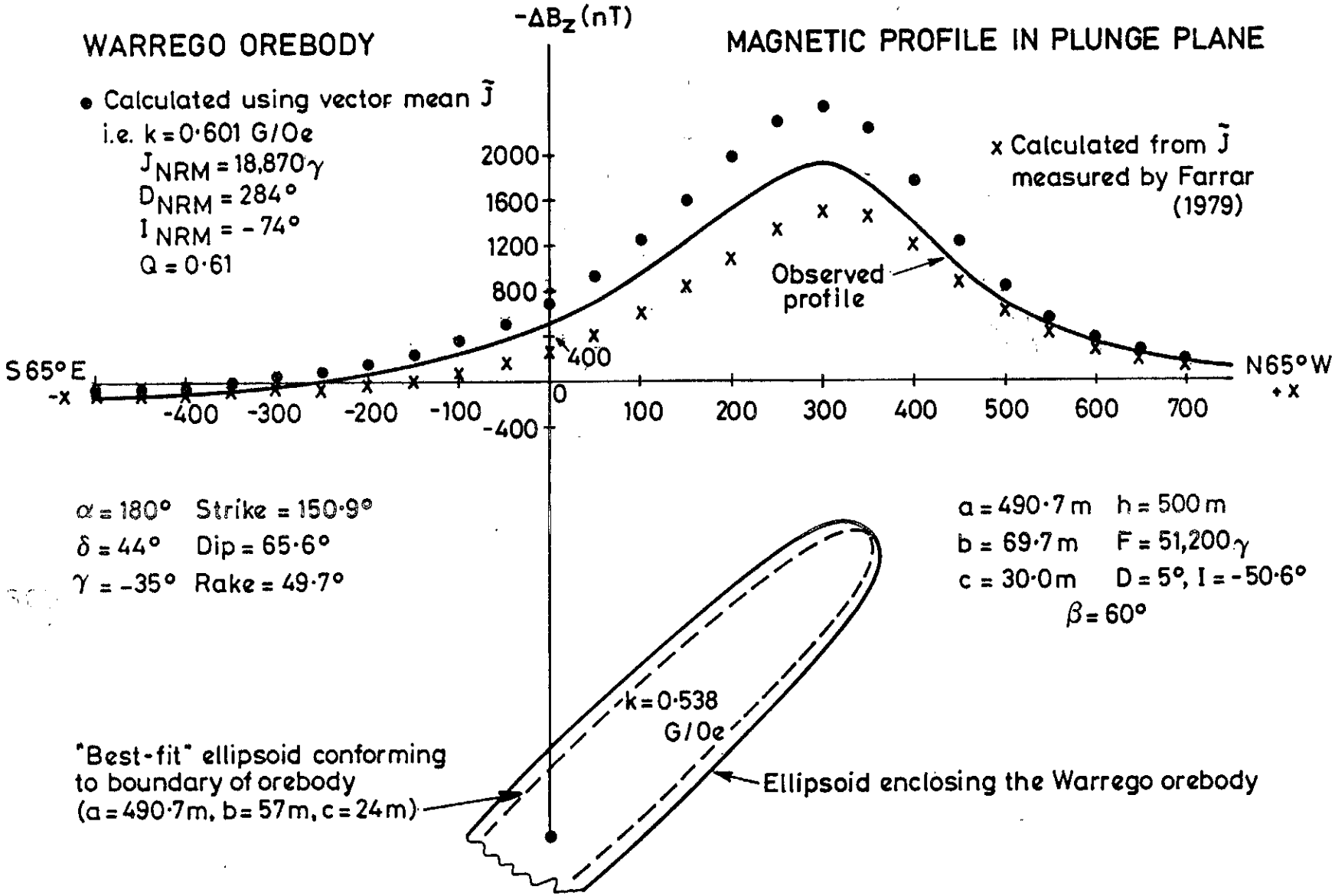
WARREGO OREBODY
• Calculated using vector mean J̃
i.e. k = 0·601 G/Oe
J_{NRM} = 18,870γ
D_{NRM} = 284°
I_{NRM} = -74°
Q = 0·61
-ΔBz (nT)
MAGNETIC PROFILE IN PLUNGE PLANE
x Calculated from J̃ measured by Farrar (1979)
Observed profile
2000
1600
1200
800
400
S 65° E
-x
N65° W
+x
-400
-300
-200
-100
0
100
200
300
400
500
600
700
-400
α = 180° Strike = 150·9°
δ = 44° Dip = 65·6°
γ = -35° Rake = 49·7°
a = 490·7 m h = 500 m
b = 69·7 m F = 51,200γ
c = 30·0 m D = 5°, I = -50·6°
β = 60°
k = 0·538 G/Oe
"Best-fit" ellipsoid conforming to boundary of orebody (a = 490·7m, b = 57m, c = 24m)
Ellipsoid enclosing the Warrego orebody

FIG.2

FIG. 3 Zijderveld plots for representative specimens from the Warrego ironstone. Closed symbols represent vector end-points projected onto the horizontal plane and open symbols represent the corresponding projections onto a vertical plane. Successive points correspond to remanence vectors measured after palaeomagnetic cleaning treatment (AF or thermal demagnetisation).

specimen is
war 1A2

step	dec	inc	inten
plot starts from here			
NRM	89	-68	7.3999e+04
5 OE	89	-72	7.6298e+04
_0 OE	85	-69	6.4962e+04
15 OE	84	-72	5.1633e+04
20 OE	97	-73	5.0239e+04
40 OE	91	-66	2.8397e+04
b0 OE	88	-71	1.3005e+04
80 OE	79	-78	6.9475e+03
100 OE	83	-80	3.2602e+03
150 OE	348	-82	8.8625e+02

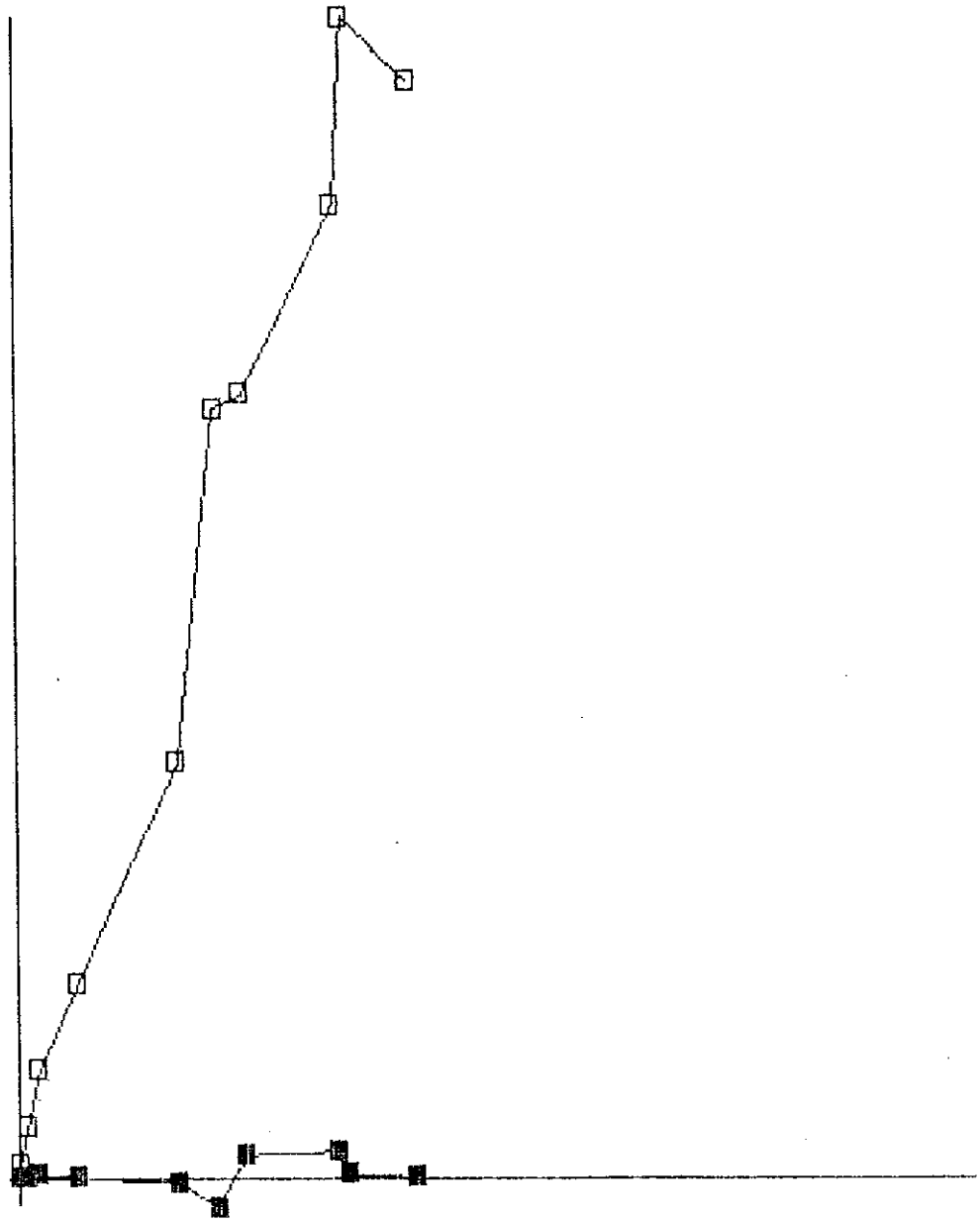

FIG.3

specimen is
war 1A3

step	dec	inc	inten
plot starts from here			
NRM	324	-45	2.1264e+04
100 C	317	-58	1.9688e+04
130 C	311	-57	1.8658e+04
160 C	311	-59	1.7666e+04
190 C	315	-60	1.6720e+04
230 C	311	-61	1.6638e+04
250 C	306	-61	1.5377e+04
290 C	213	-61	2.4830e+04
310 C	218	-60	2.3498e+04
330 C	218	-55	2.0802e+04
350 C	219	-56	1.8854e+04
370 C	216	-55	1.6841e+04
390 C	220	-53	1.4763e+04
410 C	227	-49	1.3142e+04
450 C	224	-52	1.1466e+04

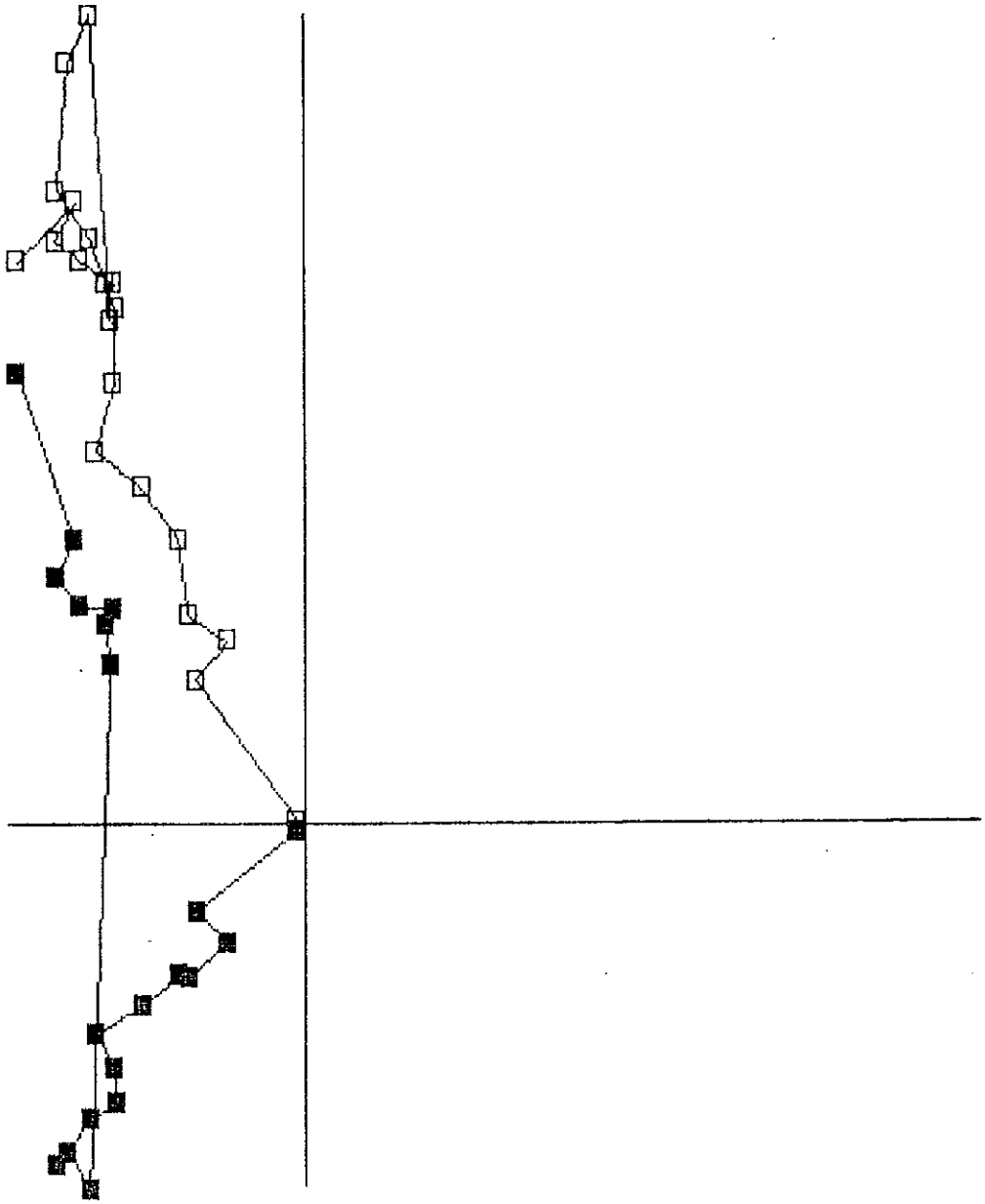

specimen is
war 3A3

step	dec	inc	inten
370 C	344	-4	4.2561e+03
390 C	345	-4	3.9149e+03
410 C	345	-5	3.7106e+03
450 C	345	-4	3.3710e+03
500 C	344	-5	2.9061e+03
550 C	346	-3	2.0432e+03
570 C	346	-4	1.7045e+03
580 C	345	-5	1.3203e+03
600 C	336	-2	5.1749e+02
630 C	314	-15	1.3255e+02
230 C	345	-4	5.8384e+03
250 C	347	-2	5.5326e+03
290 C	348	-8	5.1098e+03
310 C	345	-5	5.0328e+03
330 C	344	-5	4.7887e+03
350 C	344	-4	4.5345e+03

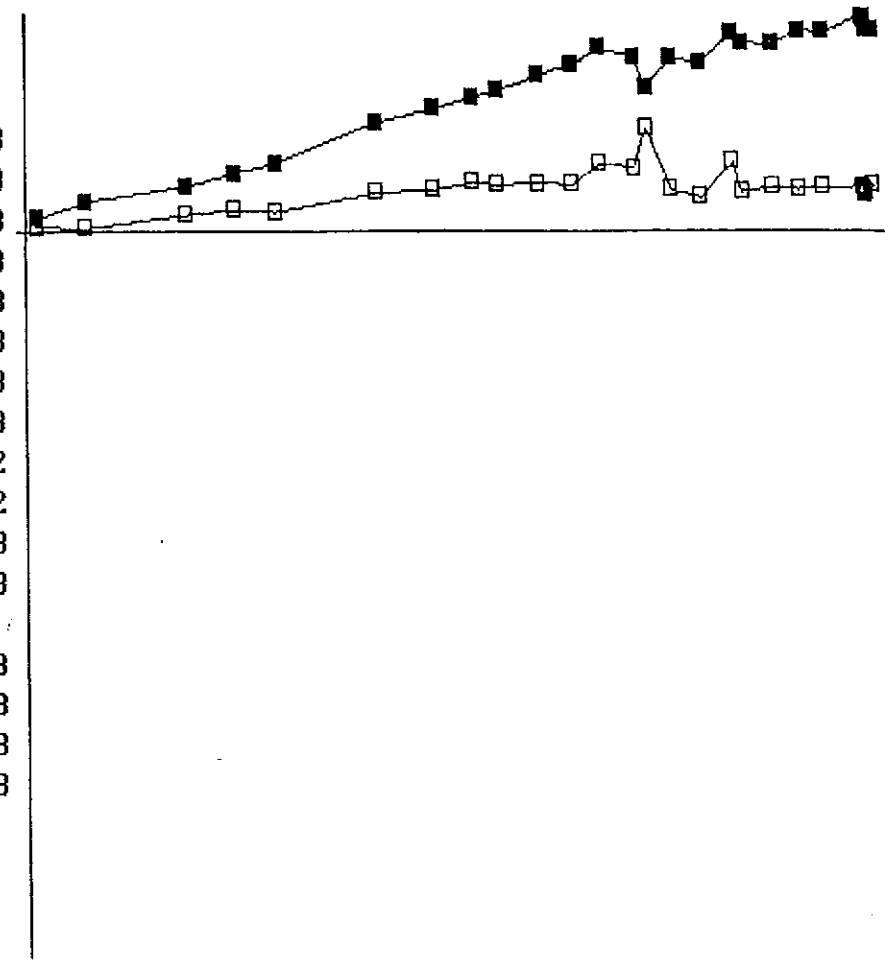

FIG. 4 Soft remanence components carried by Warrego ironstone specimens. The components were isolated by palaeomagnetic cleaning and defined using Principal Component Analysis. The diamond represents the present field direction in this and following figures.

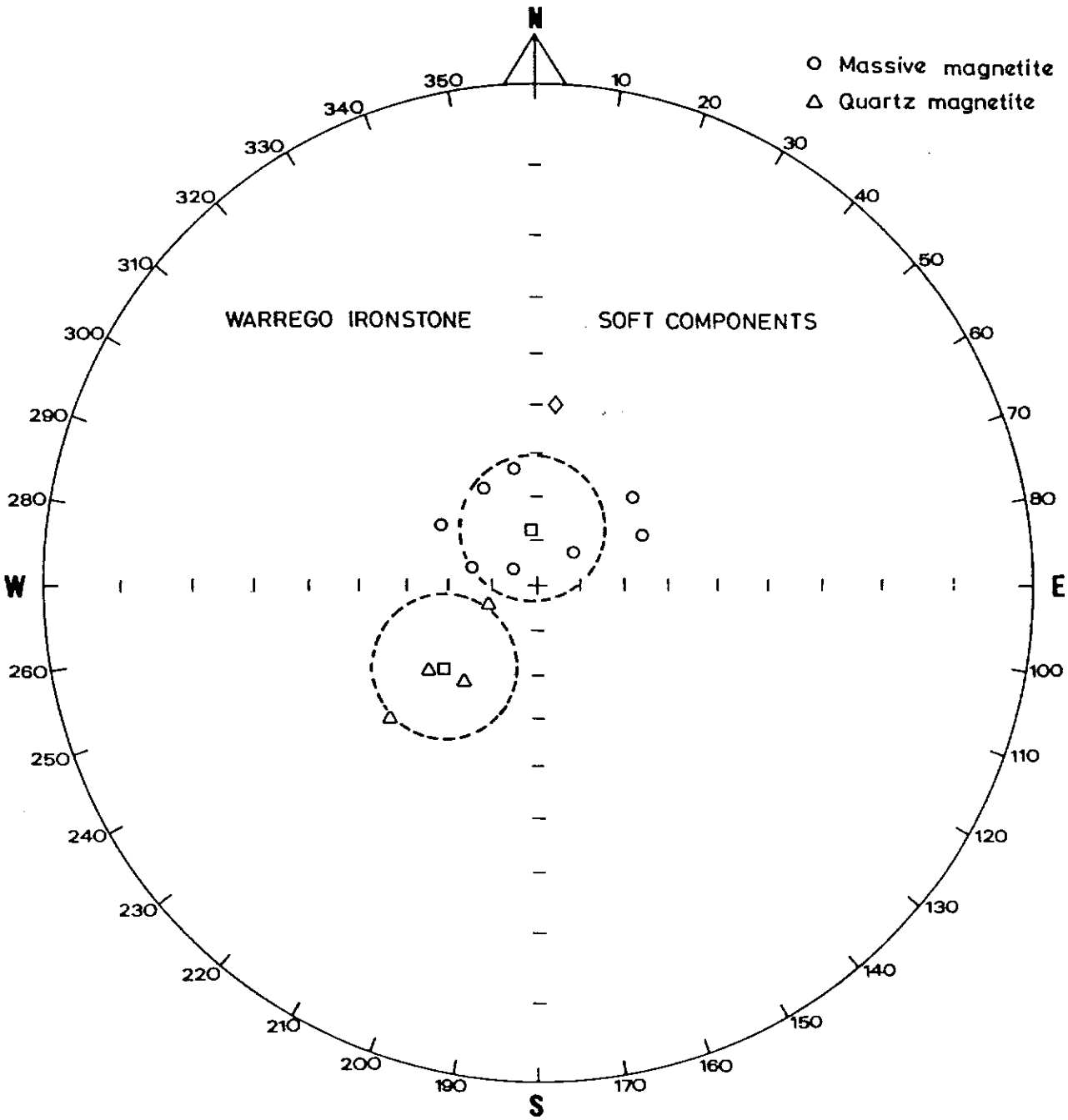
N
S
E
W
10
20
30
40
50
60
70
80
100
110
120
130
140
150
160
170
190
200
210
220
230
240
250
260
280
290
300
310
320
330
340
350
O Massive magnetite
Δ Quartz magnetite
WARREGO IRONSTONE
SOFT COMPONENTS

FIG. 4

FIG. 5 Hard remanence components isolated from Warrego ironstone specimens.

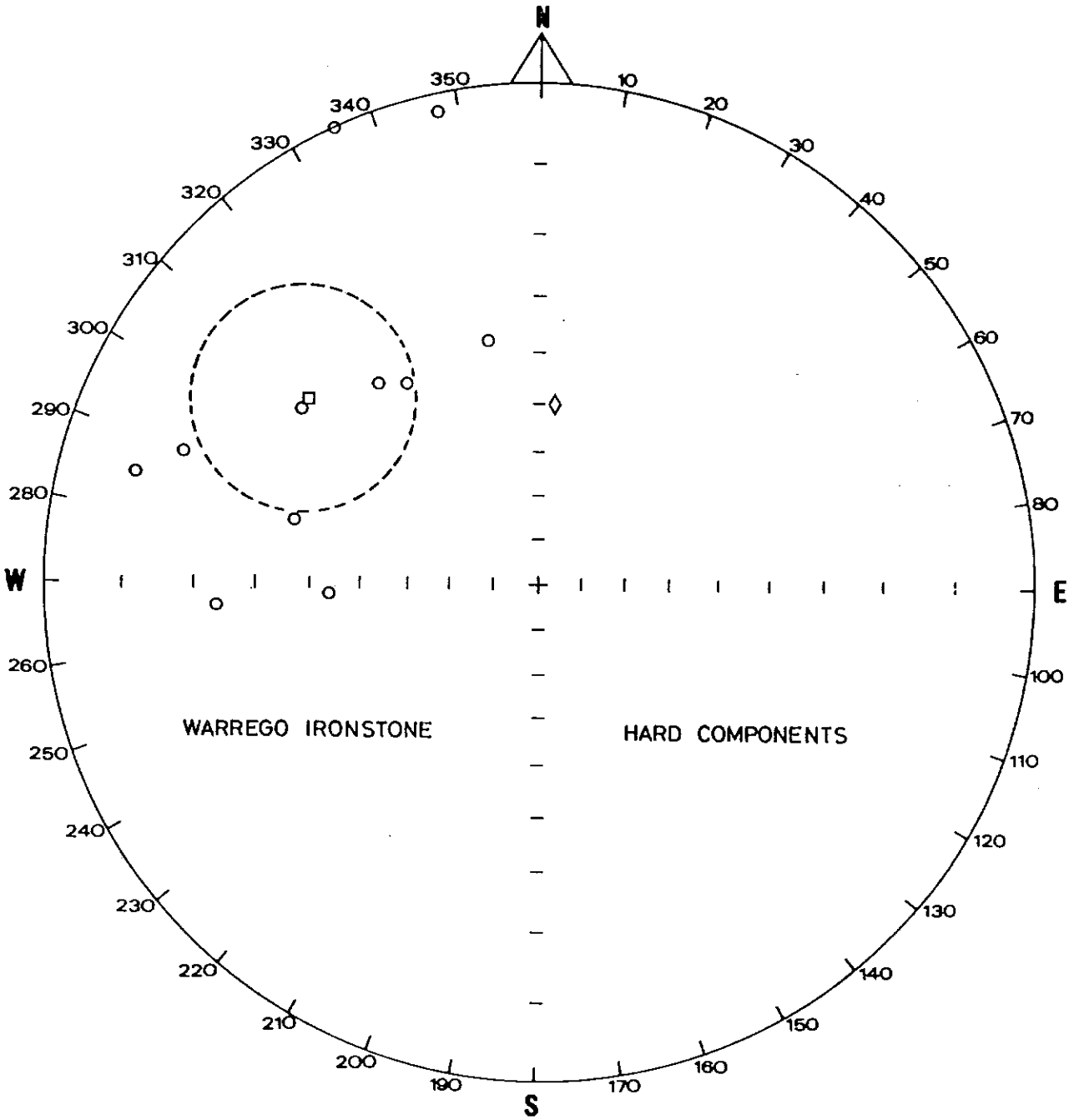
N
E
S
W
10
20
30
40
50
60
70
80
100
110
120
130
140
150
160
170
190
200
210
220
230
240
250
260
280
290
300
310
320
330
340
350
WARREGO IRONSTONE
HARD COMPONENTS

FIG.5

FIG. 6 NRM directions of host rock specimens from the Explorer 50 prospect, plotted on an equal angle stereonet.

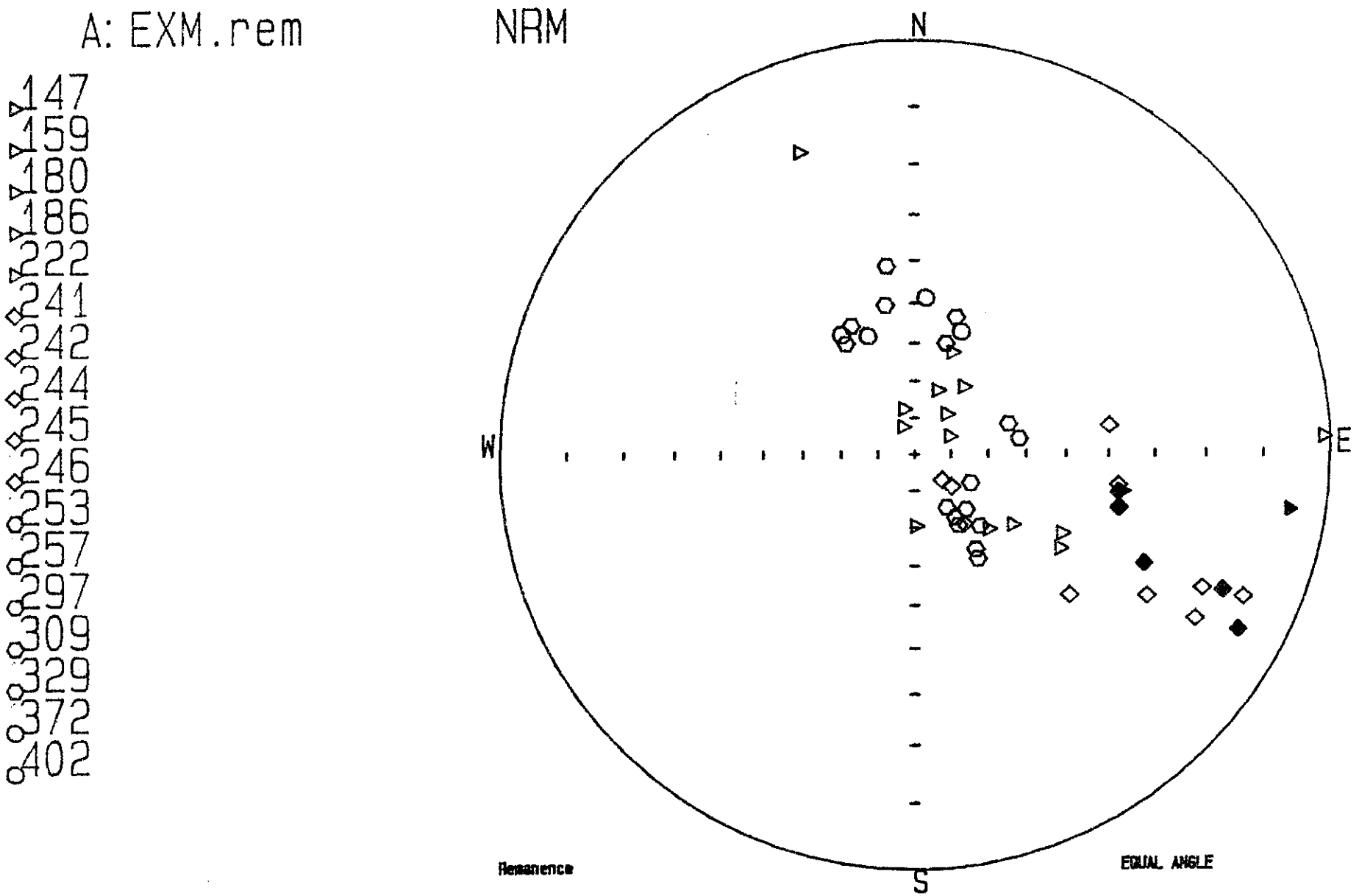
A: EXM.rem
NRM
147
159
180
186
222
241
242
244
245
246
253
257
297
309
329
372
402
N
W
E
S
Remanence
EQUAL ANGLE

FIG.6

FIG. 7 Magnetic fabric of Explorer 50 host rock samples. Lamprophyre samples are indicated by bars on the plotted susceptibility axes. Equal area projection.

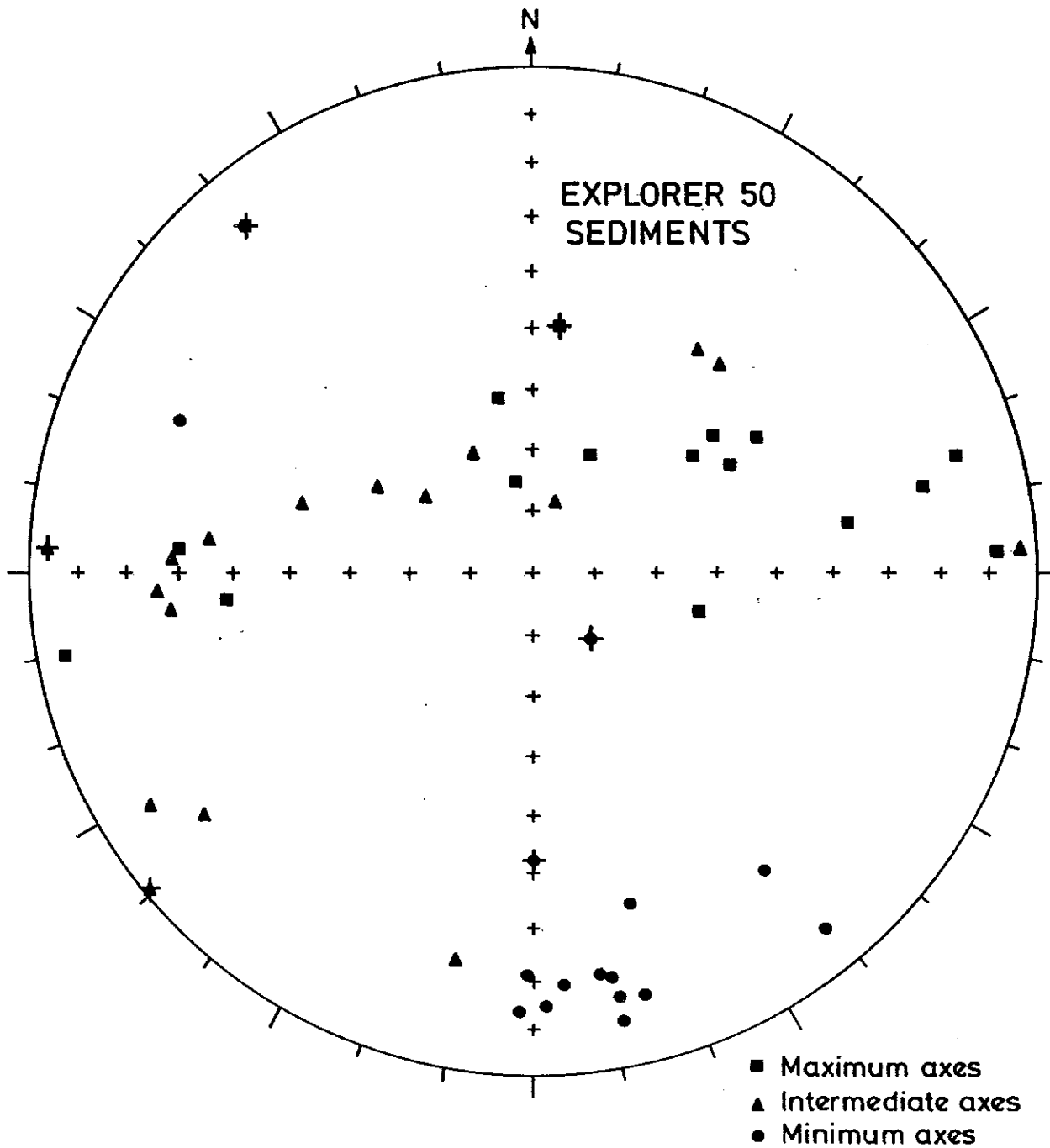
N
EXPLORER 50
SEDIMENTS
Maximum axes
Intermediate axes
Minimum axes

FIG.7

FIG. 8 Zijderveld plots for representative sedimentary specimens from Explorer 50.

specimen is

exm 180

step	dec	inc	inten
570 C	82	40	1.0276e+01
580 C	85	38	4.7500e+00
VRM	74	29	2.7575e+01
20 OE	79	31	2.7841e+01
60 OE	78	35	2.6608e+01
80 OE	79	35	2.6774e+01
100 OE	78	36	2.6521e+01
200 C	81	41	2.6163e+01
250 C	84	41	2.6560e+01
300 C	81	41	2.5816e+01
350 C	85	42	2.6100e+01
400 C	81	42	2.4873e+01
450 C	83	42	2.4276e+01
500 C	87	40	2.1542e+01
550 C	86	41	1.4867e+01
560 C	86	41	1.1266e+01

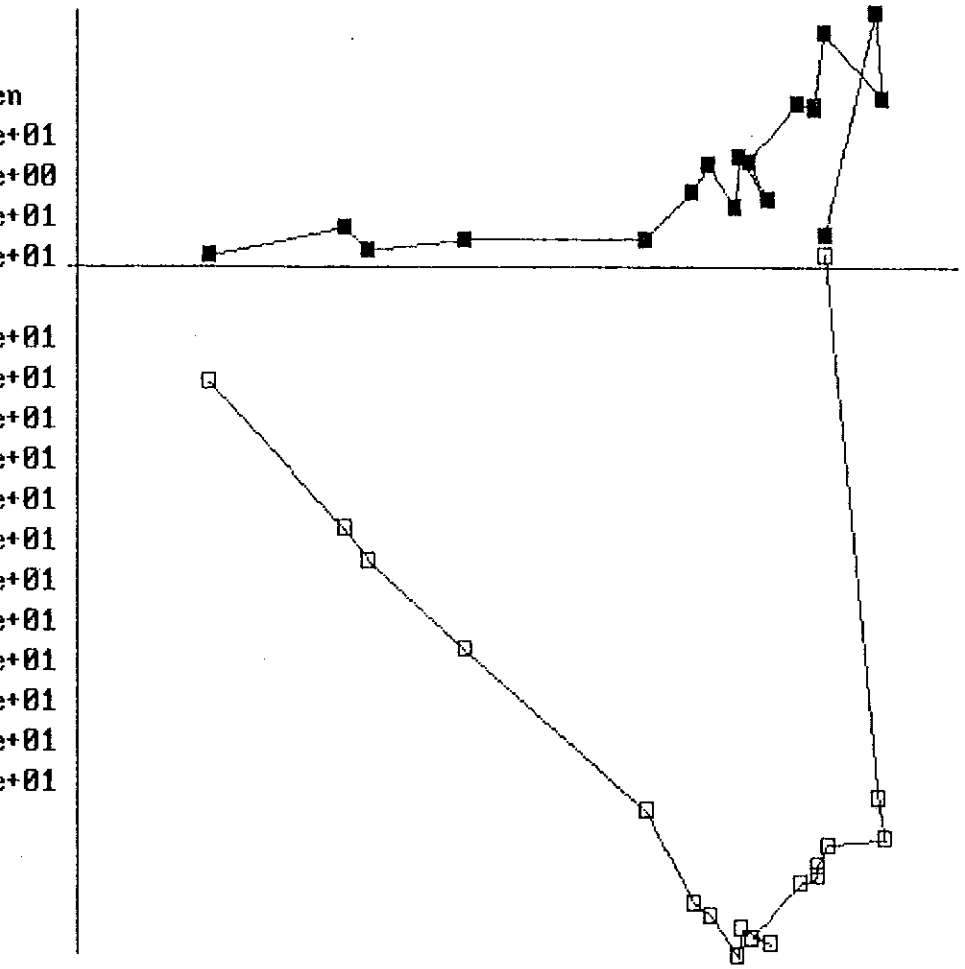

FIG.8

specimen is
exm 241B

step	dec	inc	inten
plot starts from here			
NRM	120	-13	3.0027e+02
VRM	118	-9	2.7992e+02
200 C	128	20	2.6830e+02
250 C	129	28	2.4547e+02
300 C	134	30	2.7822e+02
350 C	127	33	2.7971e+02
400 C	126	38	2.7703e+02
450 C	124	36	2.8202e+02
500 C	120	41	2.7054e+02
550 C	124	42	2.4696e+02
560 C	119	42	2.3991e+02
570 C	120	41	1.3390e+02
580 C	120	36	5.0669e+01

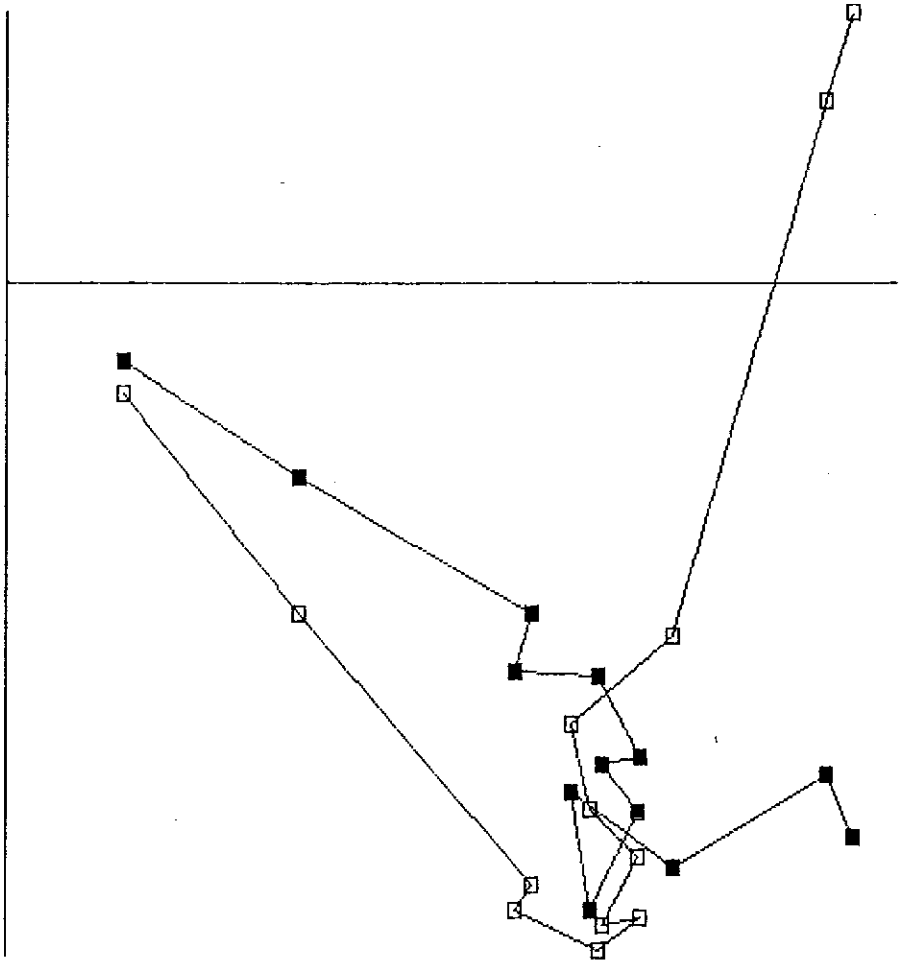

Down South

specimen is
exm 242C

step	dec	inc	inten
plot starts from here			
NRM	115	-15	1.5672e+02
VRM	113	-13	1.4564e+02
20 OE	111	-10	1.3110e+02
40 OE	109	-3	1.0517e+02
60 OE	114	5	9.6660e+01
80 OE	112	15	8.9511e+01
100 OE	108	21	8.6906e+01
200 C	107	36	8.3034e+01
250 C	110	39	8.8802e+01
300 C	109	41	8.8522e+01
350 C	110	47	9.3435e+01
400 C	112	49	9.6403e+01
450 C	110	50	9.3458e+01
500 C	94	46	9.3754e+01
550 C	107	51	8.3761e+01
560 C	107	53	7.3332e+01

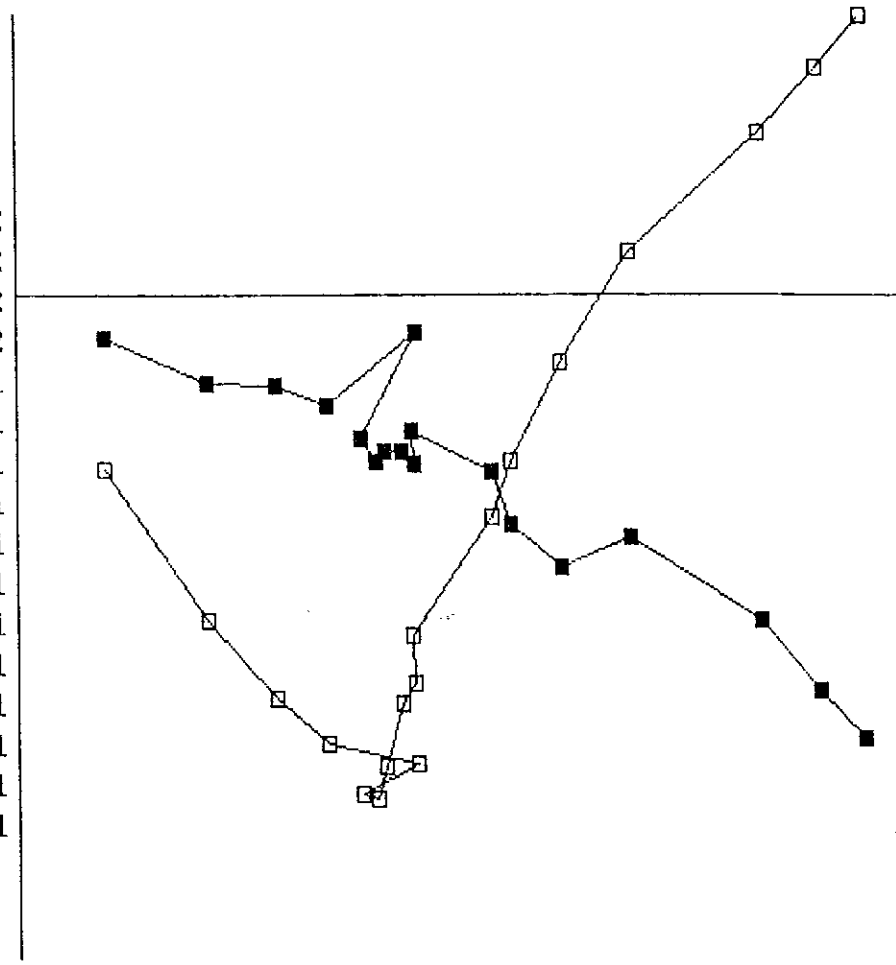

Down South

specimen is
 exm 244A
 step dec inc inten

plot starts from here

NRM	114	11	2.7482e+02
VRM	109	11	2.7251e+02
20 OE	109	20	2.6916e+02
40 OE	112	31	2.6652e+02
60 OE	100	35	2.7529e+02
80 OE	110	40	2.9283e+02
100 OE	105	42	2.9774e+02
200 C	107	51	2.7838e+02
250 C	107	46	3.1179e+02
300 C	100	46	3.1308e+02
350 C	105	48	3.1682e+02
400 C	101	49	3.1700e+02
450 C	98	48	3.1268e+02
500 C	97	48	3.0195e+02
550 C	100	47	3.0265e+02
560 C	101	48	2.7228e+02

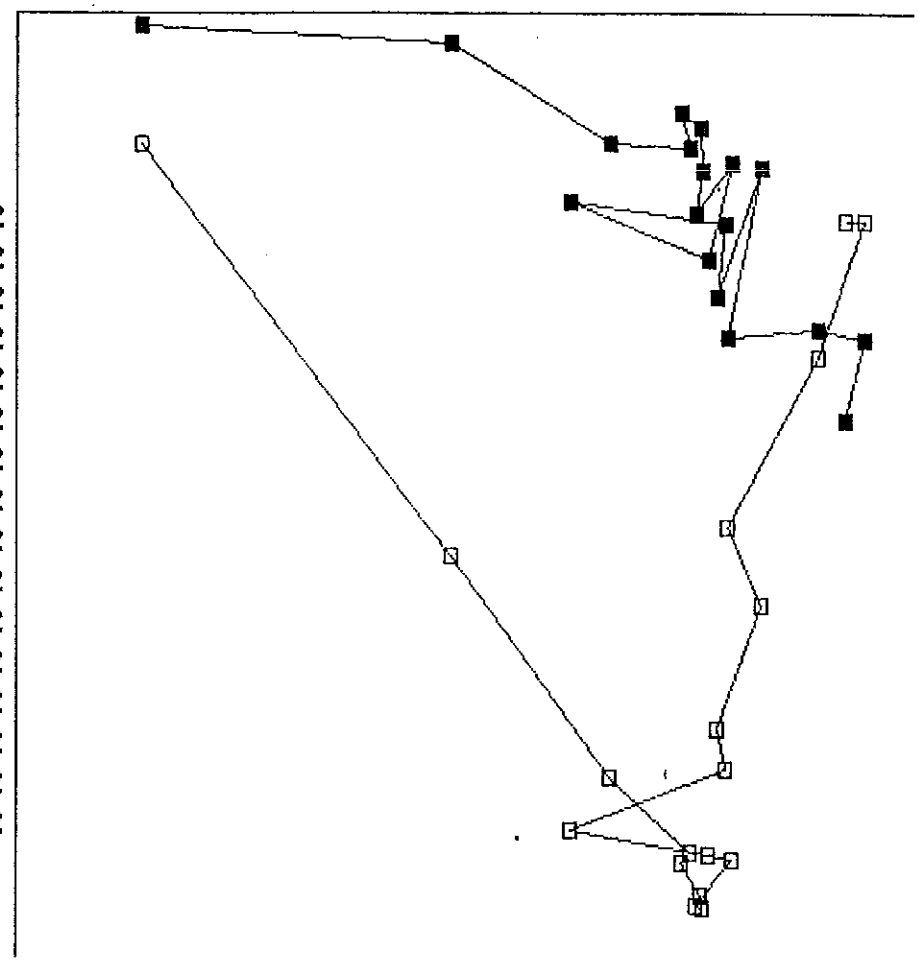

Down South

specimen is
exm 246D

step	dec	inc	inten
plot starts from here			
NRM	98	-37	4.1637e+01
VRM	96	-37	3.8725e+01
200 C	95	13	3.0288e+01
50 OE	88	27	3.3510e+01
100 OE	89	40	3.8886e+01
150 OE	87	46	4.2563e+01
200 OE	76	53	4.1605e+01
250 OE	84	52	4.1539e+01
300 OE	85	52	3.8851e+01
350 OE	81	52	3.4635e+01
400 OE	85	53	3.1391e+01
450 OE	84	52	2.7858e+01
500 OE	86	54	2.2081e+01
550 OE	84	53	1.4381e+01
600 OE	81	57	1.2433e+01
650 OE	86	55	1.0955e+01

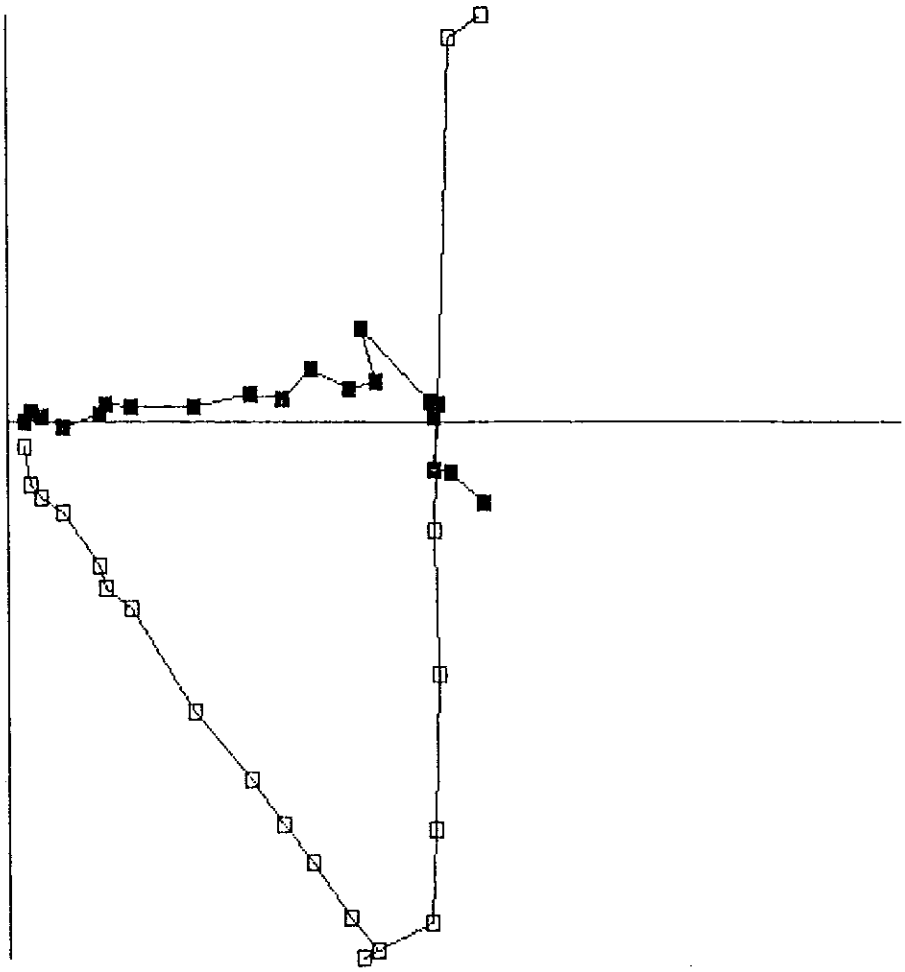

Down South

FIG. 9 Soft remanence components isolated from Explorer 50 sediment samples. Equal angle projection.

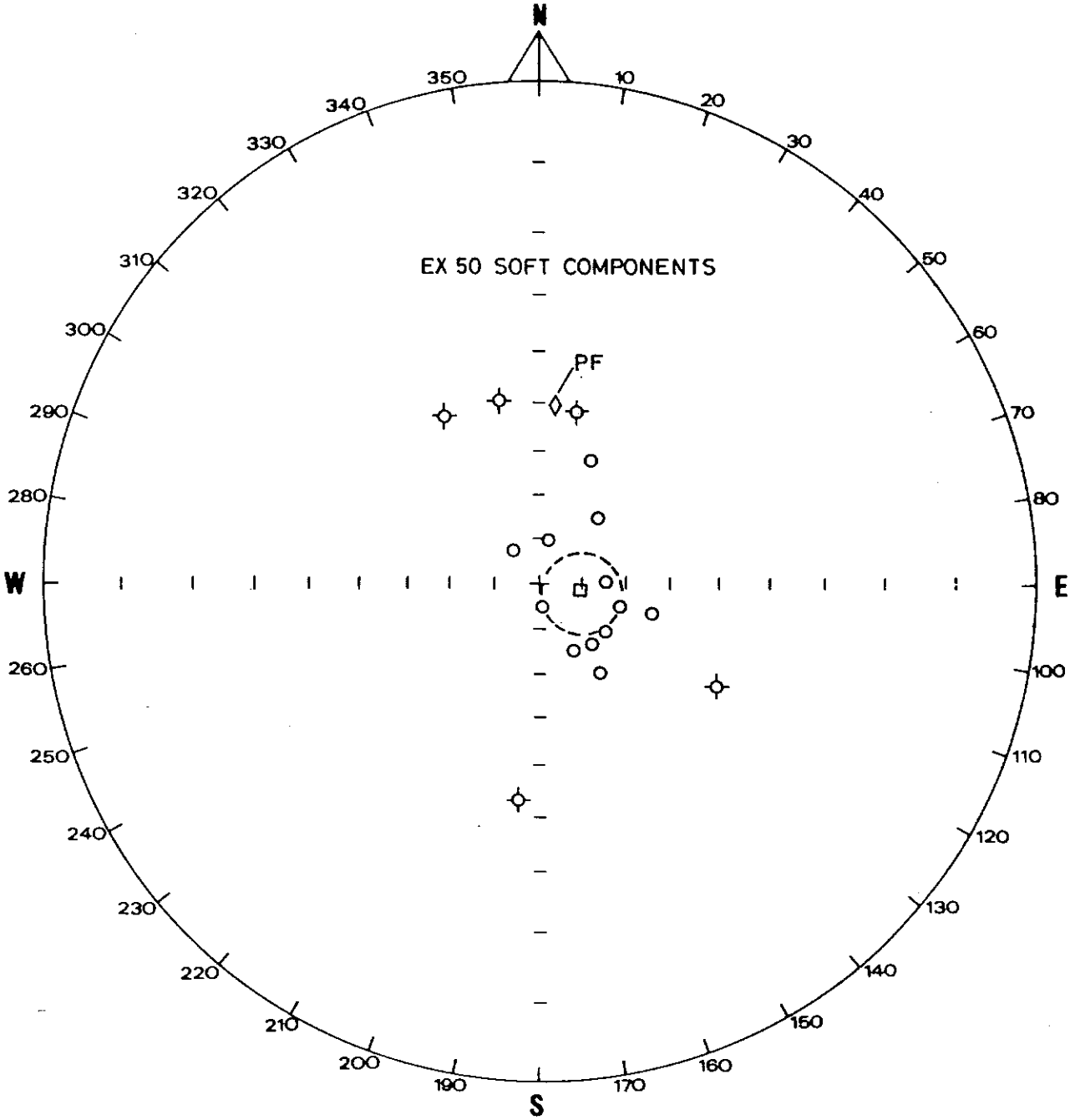
N
350
10
20
30
340
330
320
40
310
50
EX 50 SOFT COMPONENTS
300
60
PF
290
70
280
80
W
E
260
100
250
110
240
120
230
130
220
140
210
150
200
160
190
170
S

FIG.9

FIG. 10 Hard remanence components isolated from Explorer 50 sediment samples. Equal angle projection.

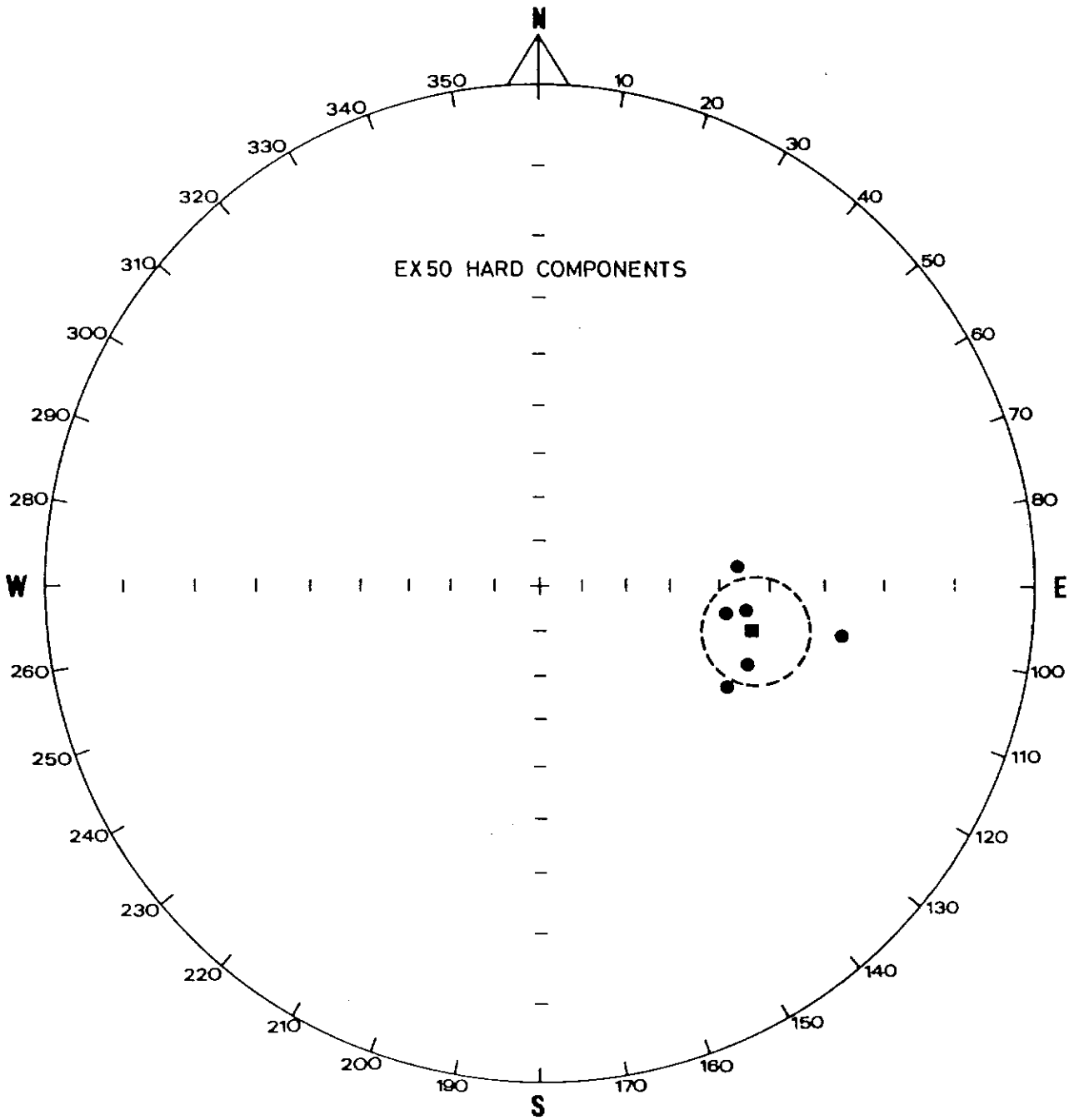
N
E
S
W
EX 50 HARD COMPONENTS
10
20
30
40
50
60
70
80
100
110
120
130
140
150
160
170
190
200
210
220
230
240
250
260
280
290
300
310
320
330
340
350

FIG.10

FIG. 11 Palaeopole positions corresponding to the hard and soft remanence components from Explorer 50. The 1.8-0.6 Ga Precambrian apparent polar wander path for Australia (after Idnurm and Giddings, 1987) is shown for comparison. The dashed circles represent 95% cones of confidence about the pole positions. The corresponding antipoles are indicated in parentheses.

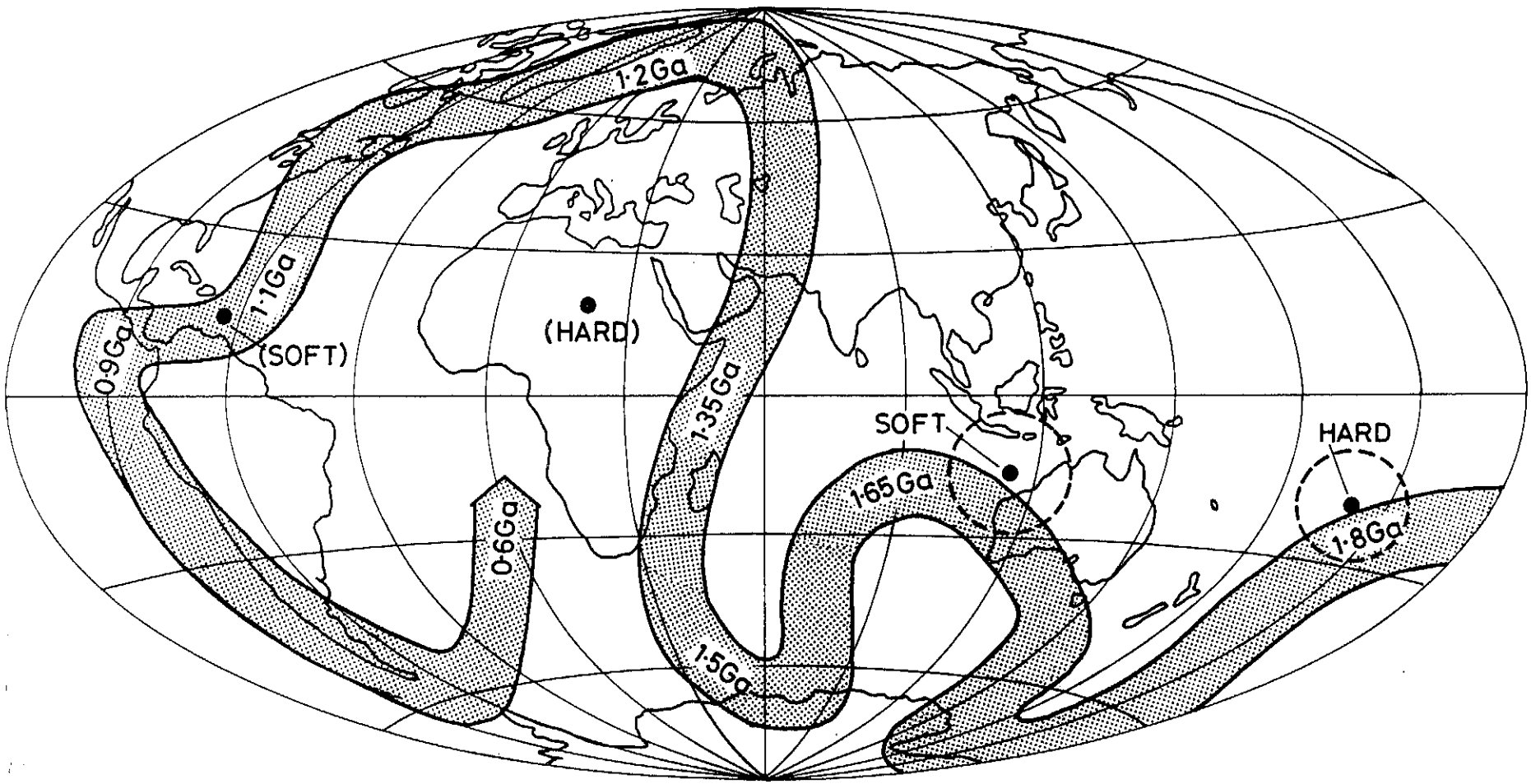
1·2Ga
1·1Ga
0·9Ga
(SOFT)
(HARD)
1·35Ga
0·6Ga
1·5Ga
SOFT
1·65Ga
HARD
1·8Ga

FIG.11

FIG. 12 Soft remanence components from Argo ironstone specimens. Equal angle projection.

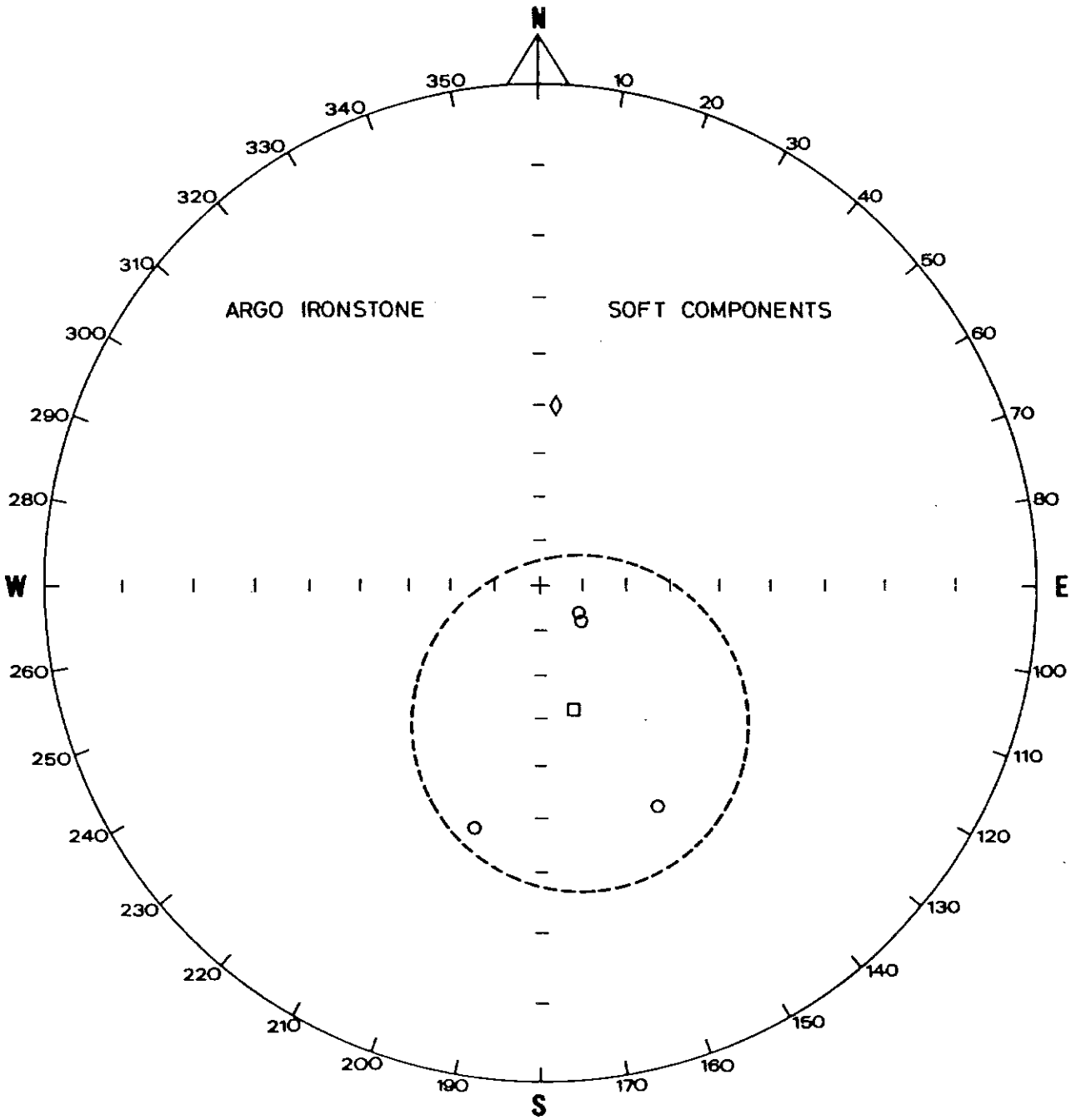
N
S
E
W
350
10
20
30
40
50
60
70
80
100
110
120
130
140
150
160
170
190
200
210
220
230
240
250
260
280
290
300
310
320
330
340
ARGO IRONSTONE
SOFT COMPONENTS

FIG.12

FIG. 13 Magnetic fabric of the Argo mine sediment samples. Equal area projection.

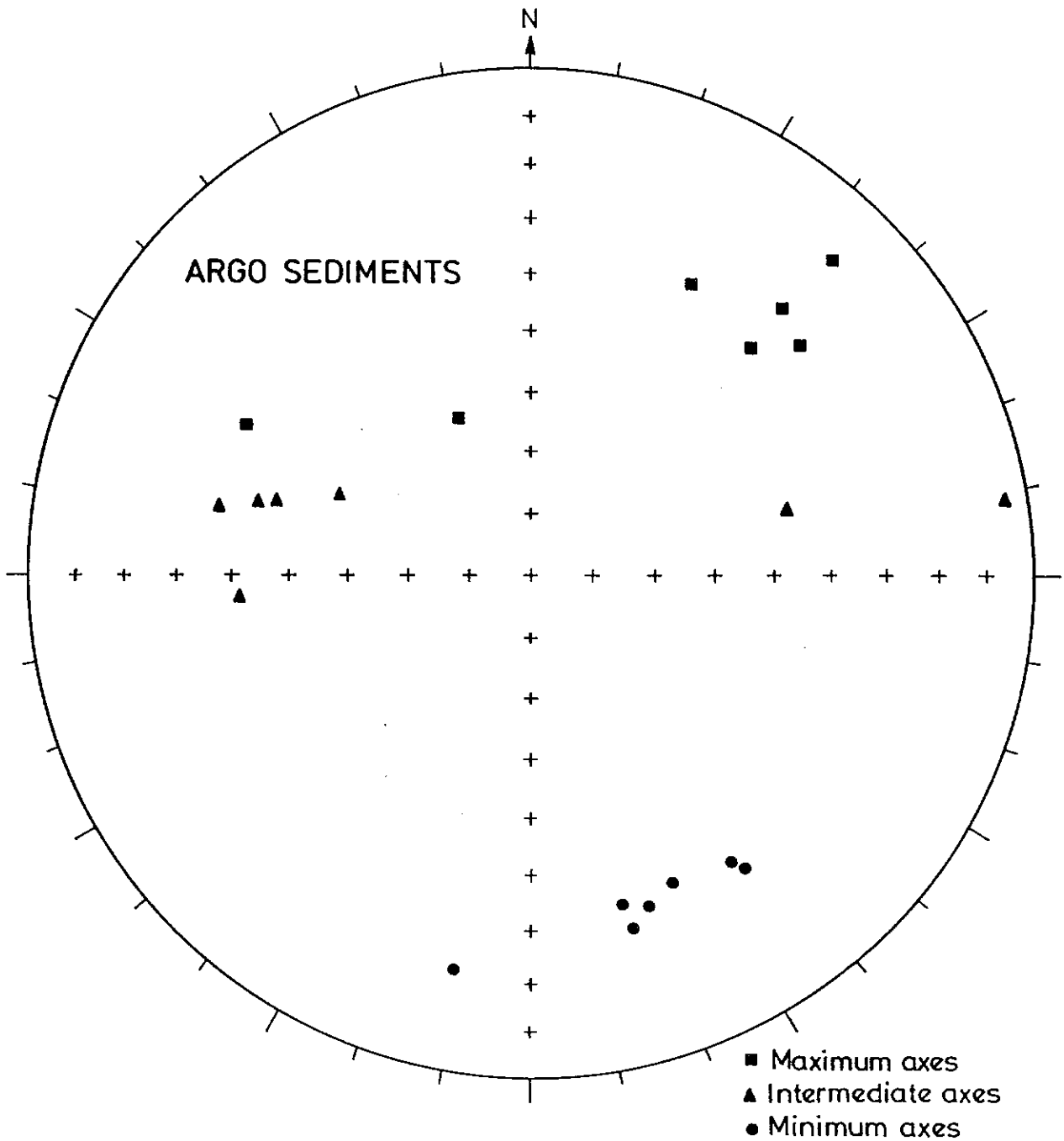
N
ARGO SEDIMENTS
Maximum axes
Intermediate axes
Minimum axes

FIG.13

FIG. 14 Magnetic fabric of specimens from Explorer 46 sediment samples. Equal area projection.

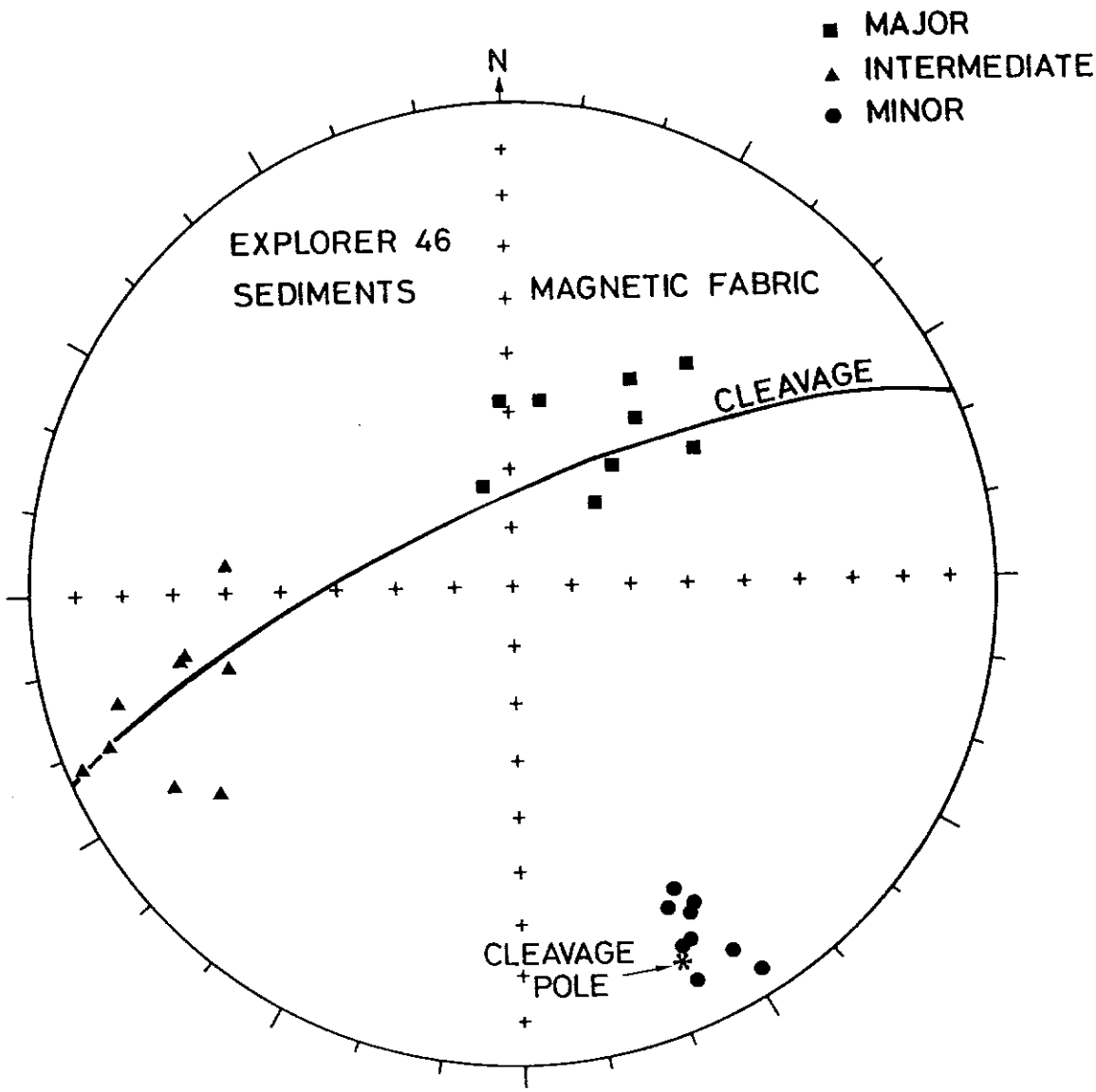
MAJOR
INTERMEDIATE
MINOR
N
EXPLORER 46
SEDIMENTS
MAGNETIC FABRIC
CLEAVAGE
CLEAVAGE
POLE

FIG.14

FIG. 15 Magnetic model for the West Gibbet ironstone.

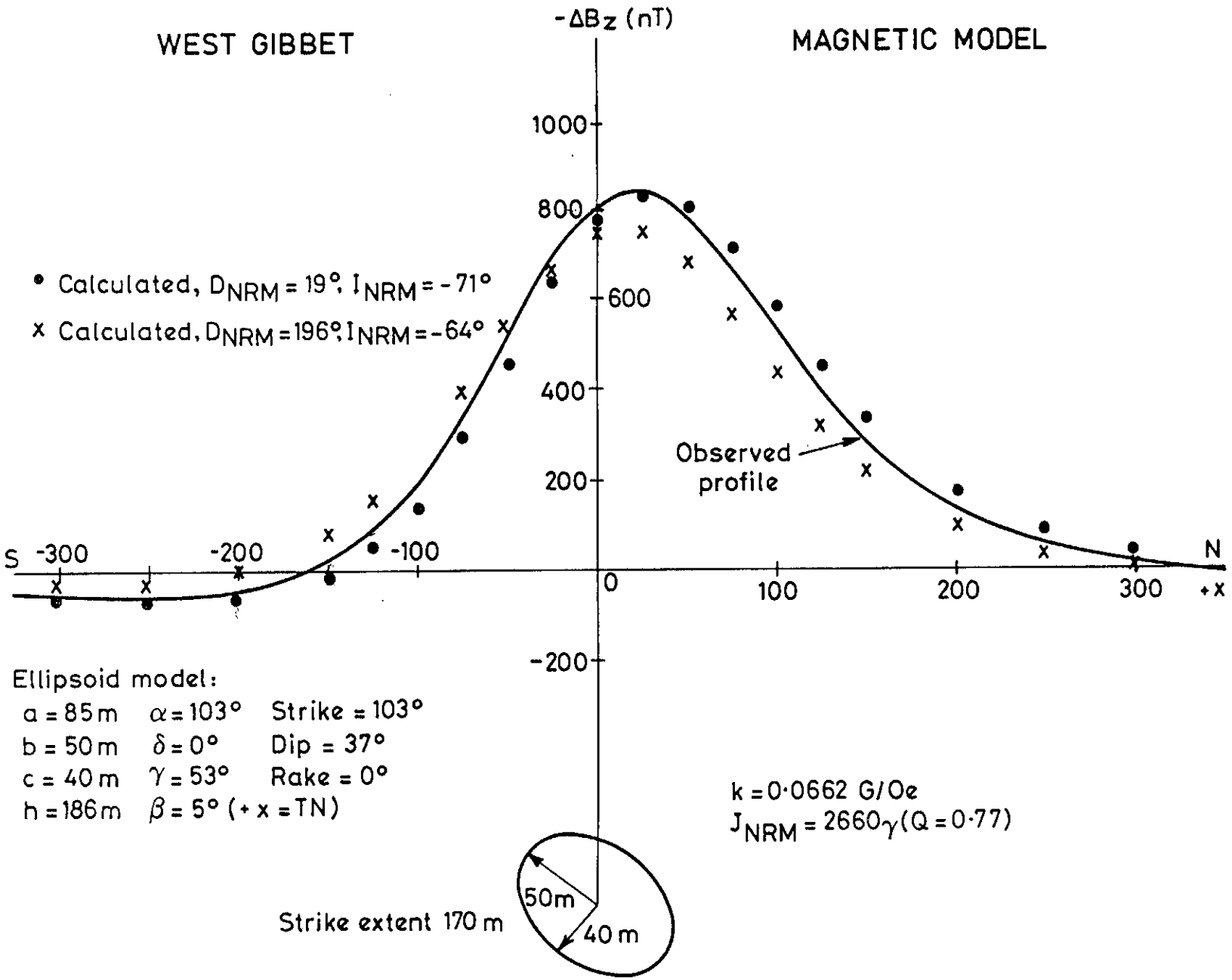
WEST GIBBET
MAGNETIC MODEL
-ΔBz (nT)
1000
800
600
400
200
-200
• Calculated, DNRM = 19°, INRM = -71°
x Calculated, DNRM = 196°, INRM = -64°
Observed profile
S
-300
-200
-100
0
100
200
300
N
+x
Ellipsoid model:
a = 85 m α = 103° Strike = 103°
b = 50 m δ = 0° Dip = 37°
c = 40 m γ = 53° Rake = 0°
h = 186 m β = 5° (+x = TN)
k = 0·0662 G/Oe
JNRM = 2660γ (Q = 0·77)
Strike extent 170 m
50m
40 m

FIG.15

FIG. 16 Magnetic fabric of West Gibbet sediment specimens. Equal area projection.

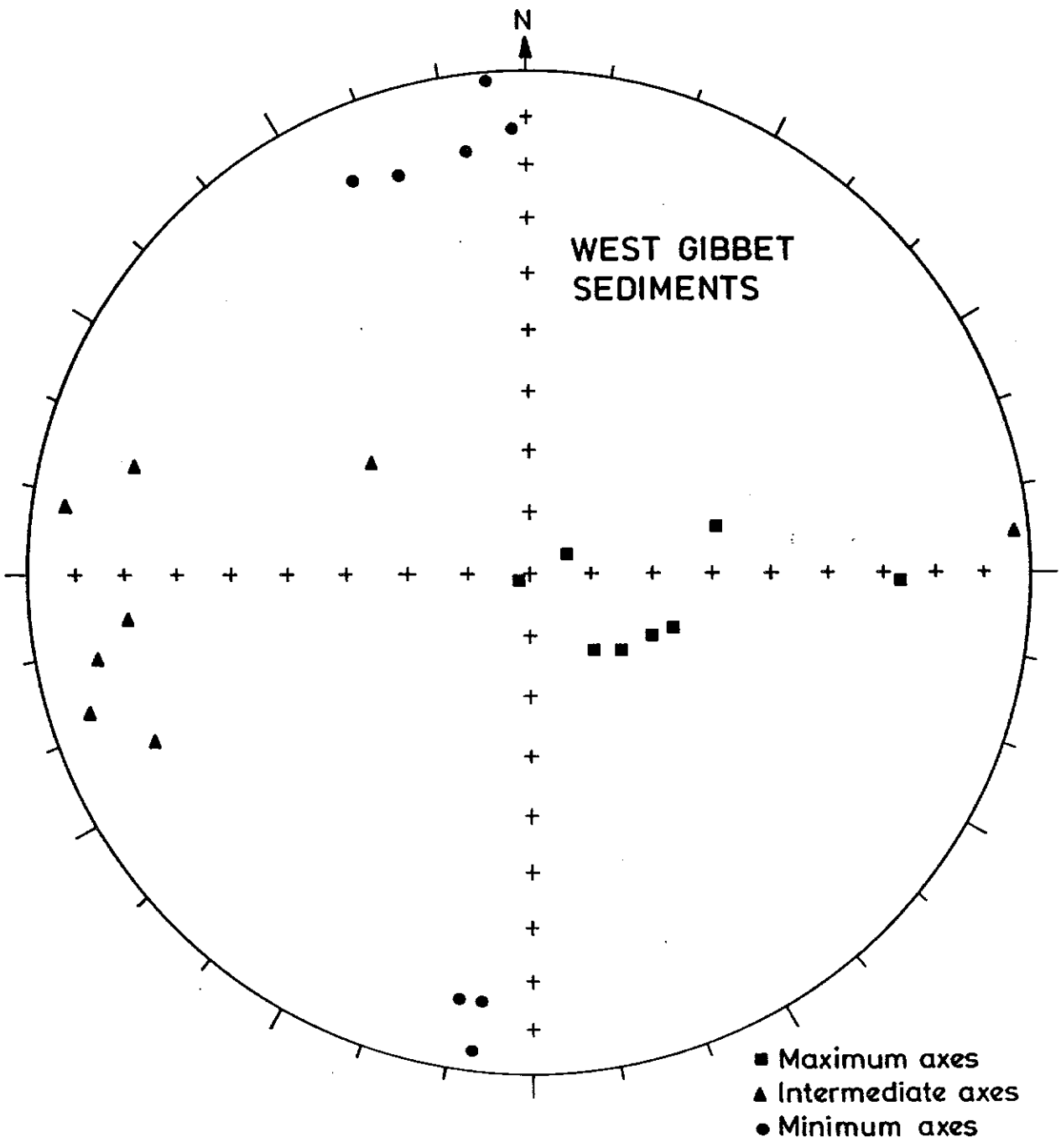
N
WEST GIBBET
SEDIMENTS
Maximum axes
Intermediate axes
Minimum axes

FIG.16

FIG. 17 Demagnetisation curve (normalised remanence intensity versus cleaning treatment) for Eldorado specimen 141B.

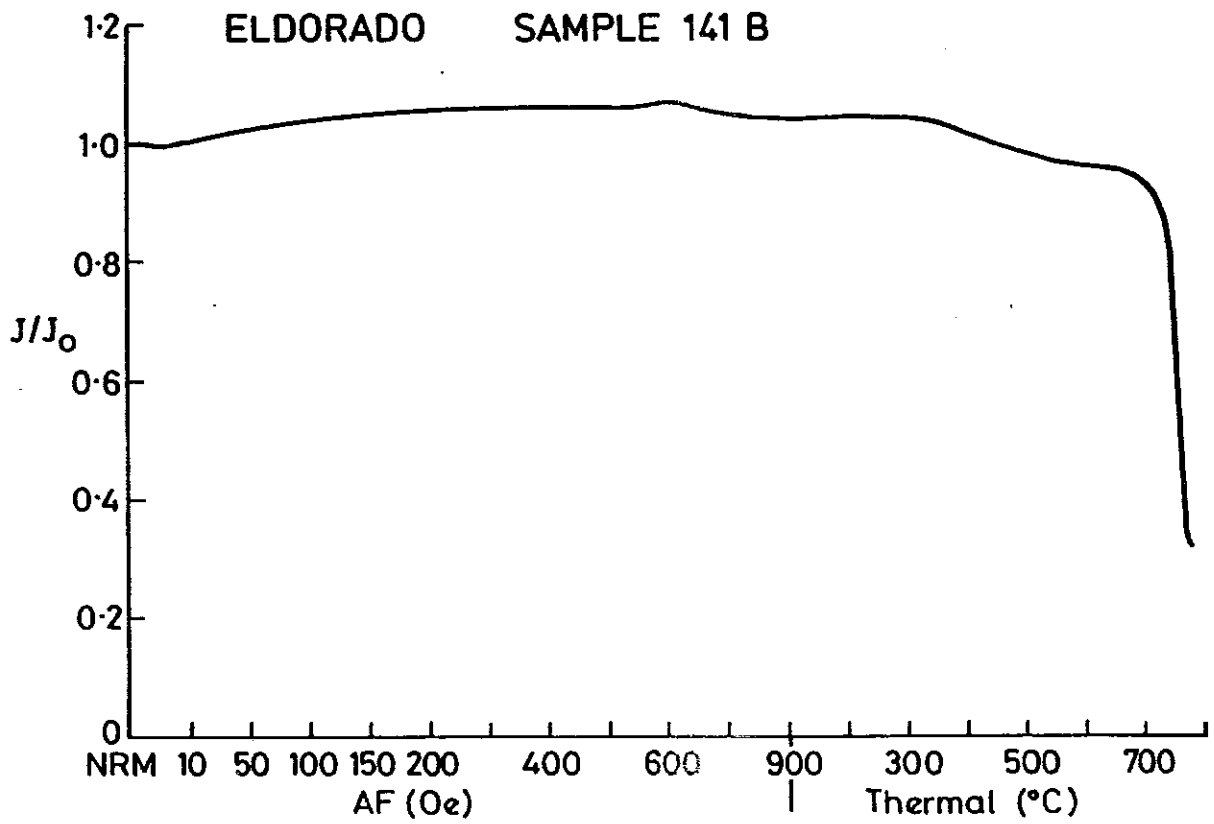
ELDORADO SAMPLE 141 B
1·2
1·0
0·8
J/J0
0·6
0·4
0·2
0
NRM 10 50 100 150 200 400 600 900 300 500 700
AF (Oe)
Thermal (°C)

FIG.17

FIG. 18 Demagnetisation curve for Eldorado specimen 186B.

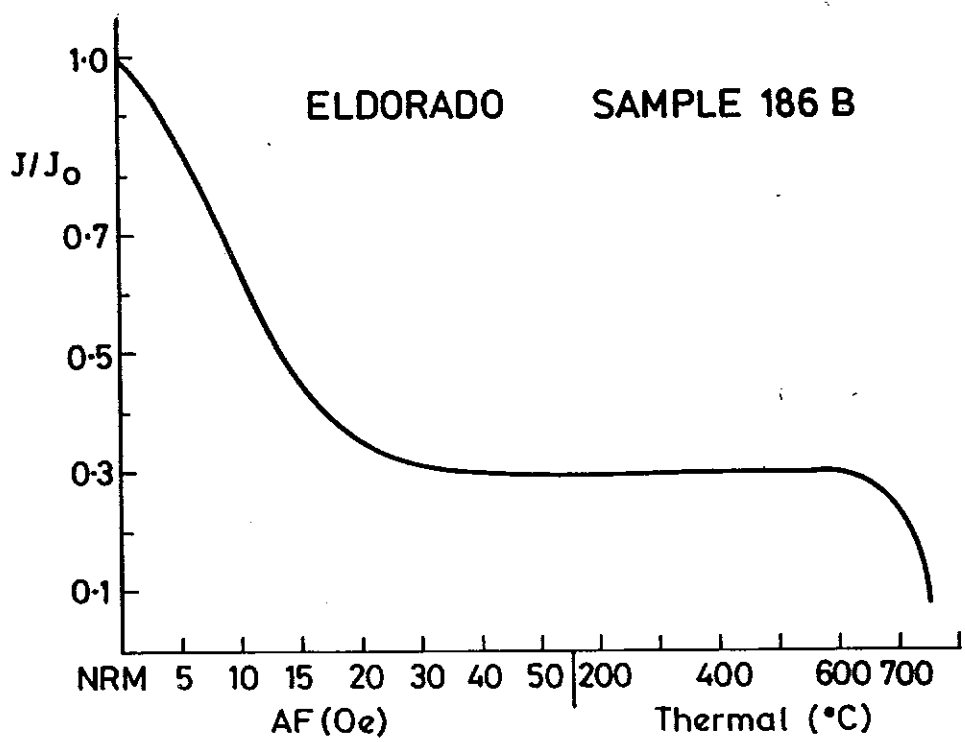
ELDORADO SAMPLE 186 B
J/J0
1·0
0·7
0·5
0·3
0·1
NRM 5 10 15 20 30 40 50 200 400 600 700
AF (Oe)
Thermal (°C)

FIG.18

FIG. 19 "Formation mean" soft remanence components carried by magnetic sediment samples.

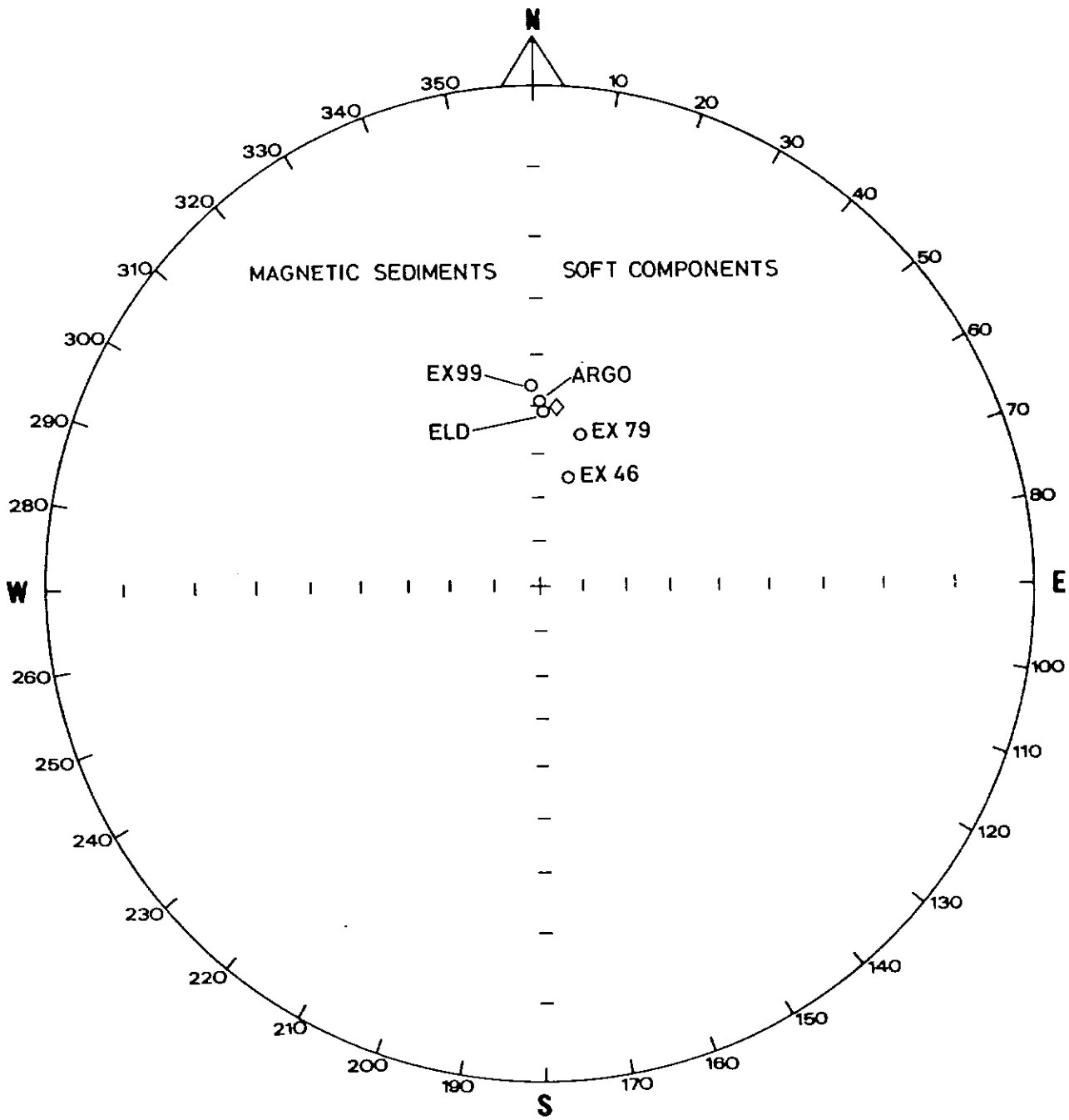
N
S
E
W
10
20
30
40
50
60
70
80
100
110
120
130
140
150
160
170
190
200
210
220
230
240
250
260
280
290
300
310
320
330
340
350
MAGNETIC SEDIMENTS
SOFT COMPONENTS
EX99
ARGO
ELD
EX 79
EX 46

FIG.19

FIG. 20 Magnetic fabric of sediment specimens from Explorer 79 and Explorer 99.

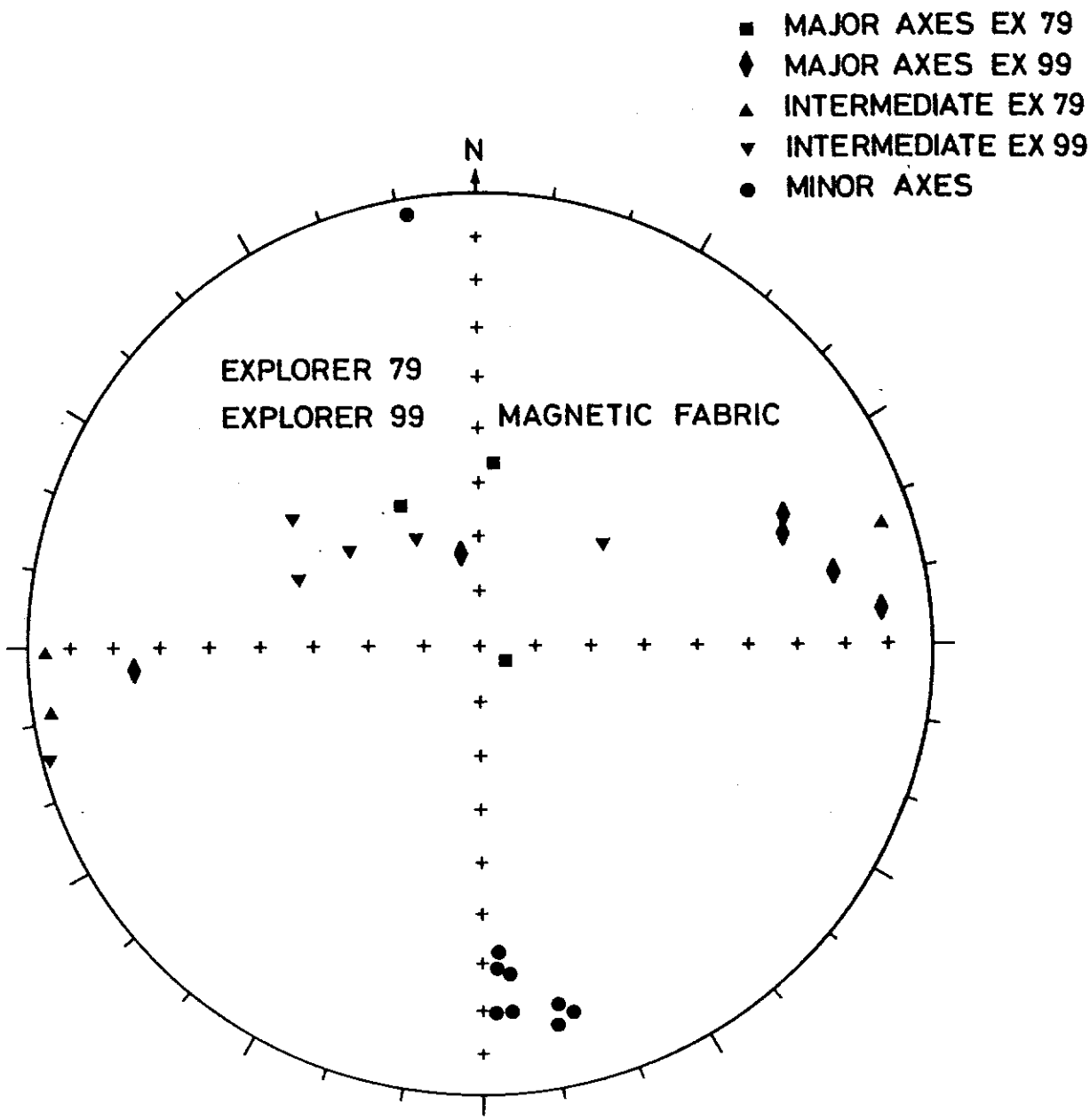
MAJOR AXES EX 79
MAJOR AXES EX 99
INTERMEDIATE EX 79
INTERMEDIATE EX 99
MINOR AXES
N
EXPLORER 79
EXPLORER 99
MAGNETIC FABRIC

FIG.20

FIG. 21 Low field thermomagnetic (susceptibility versus temperature) curves for Peko gossan samples.

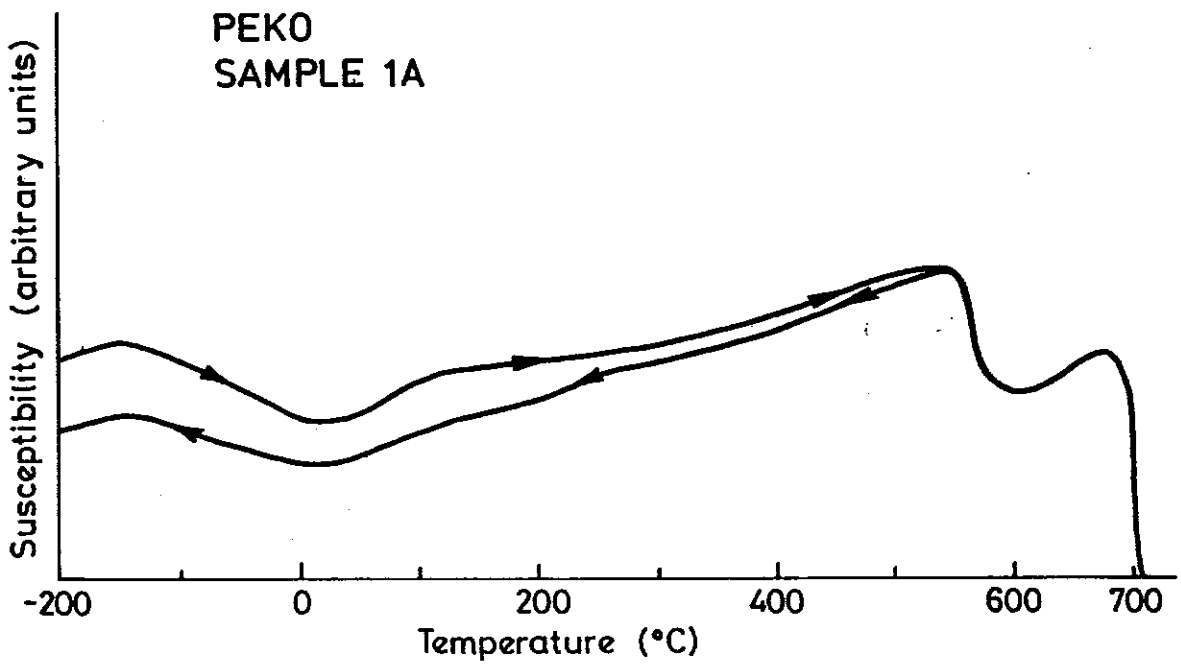
PEKO
SAMPLE 1A
Susceptibility (arbitrary units)
-200
0
200
400
600
700
Temperature (°C)

FIG.21

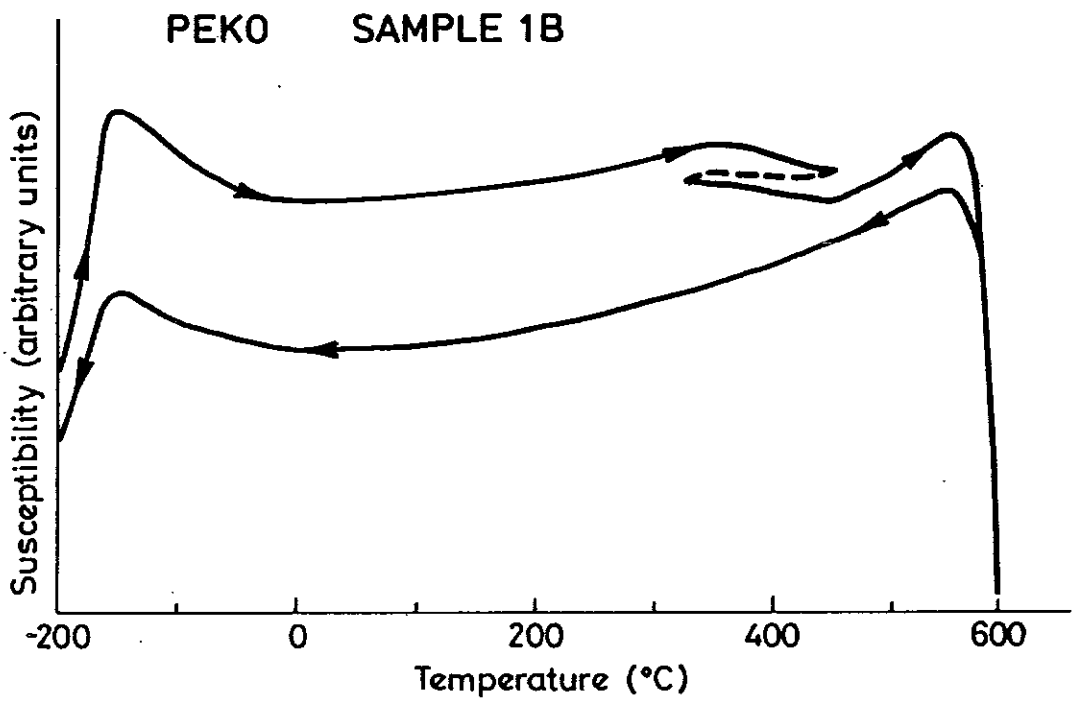
PEKO SAMPLE 1B
Susceptibility (arbitrary units)
-200
0
200
400
600
Temperature (°C)

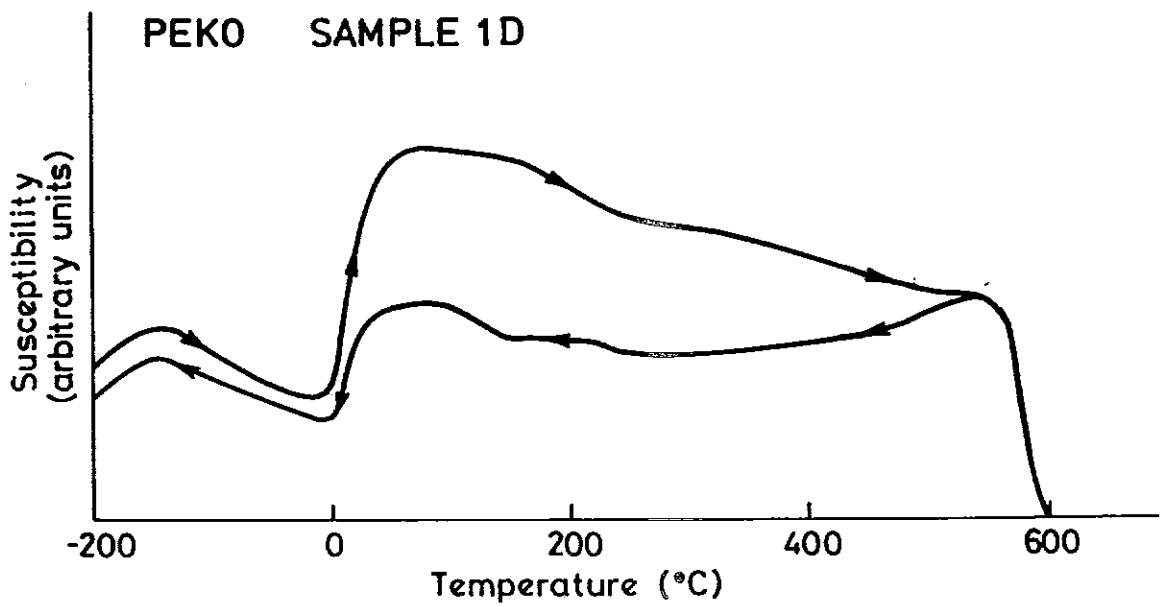
PEKO SAMPLE 1D
Susceptibility
(arbitrary units)
-200
0
200
400
600
Temperature (°C)